SIAM J. APPL. MATH.
Vol. 79, No. 6, pp. 2663–2687

SOUND PROPAGATION IN A WEAKLY TURBULENT FLOW IN A WAVEGUIDE*

LILIANA BORCEA†, JOSSELIN GARNIER‡, AND KNUT SØLNA§

Abstract. We analyze sound propagation in a waveguide filled with a random medium modeled by small-amplitude spatial and temporal fluctuations of the mass density and wave speed. The time dependence of the medium is due to a weakly turbulent flow. The analysis is based on a wave equation satisfied by the acoustic pressure, obtained by linearization of the fluid dynamic equations about the flow. The acoustic pressure is decomposed into modes, which are propagating and evanescent time-harmonic waves with amplitudes that are random fields. These amplitudes model the randomization of the sound wave due to cumulative scattering over a long distance of propagation in the random medium. We obtain a detailed statistical characterization of the mode amplitudes and use the results to solve two inverse problems: The first problem estimates the mean flow velocity from measurements of the acoustic pressure at one end of the waveguide. The second problem seeks to determine, from the same measurements, if the flow is laminar or if there is a region of turbulent flow.

Key words. random waveguides, weakly turbulent flow, wave scattering, flow estimation

AMS subject classifications. 35Q60, 35R60

DOI. 10.1137/19M1252144

1. Introduction.

We study sound propagation in a waveguide filled with a random medium that depends on time due to a flow with velocity $\boldsymbol{v}(t,\boldsymbol{x})$ that fluctuates about the mean $\langle \boldsymbol{v}(\boldsymbol{x})\rangle$. The medium is modeled by the time t and location $\boldsymbol{x}$ dependent mass density $\rho(t,\boldsymbol{x})$ and sound speed $c(t,\boldsymbol{x})$, which are random perturbations of the constant values ρ_o and c_o. The sound wave is generated by a source $\boldsymbol{F}(t,\boldsymbol{x})$ located at the origin of range, denoted by the coordinate z along the axis of the waveguide, as illustrated in Figure 1. The goal of the paper is to analyze the wave at long range, where cumulative scattering in the random medium is significant, and then use the results for estimating the flow. Specifically, given measurements of the acoustic pressure $p(t,\boldsymbol{x})$ at a remote, stationary array of receivers, we study the estimation of the mean flow and the detection and localization of a region of turbulent flow.

The classical theory of guided waves is for ideal waveguides filled with homogeneous or range-independent media and with straight and parallel reflecting boundaries [8], where the wave equation can be solved with separation of variables. The acoustic pressure field in such waveguides is a superposition of modes, which are time-harmonic propagating and evanescent waves that do not interact with each other. Their amplitudes are constant, determined by the source excitation. In waveguides filled with random media and/or with randomly fluctuating boundaries, the field $p(t,\boldsymbol{x})$ can still be decomposed into propagating and evanescent modes, but these are coupled. Their

*Received by the editors March 25, 2019; accepted for publication (in revised form) October 21, 2019; published electronically December 17, 2019.
https://doi.org/10.1137/19M1252144

Funding: The work of the first author was partially supported by the NSF grant DMS1510429, by the U.S. Office of Naval Research under award number N00014-17-1-2057, and by the AFOSR under award FA9550-18-1-0131. The work of the second author was partially supported by the French ANR under grant ANR-19-CE46-0007 (project ICCI). The work of the third author was partially supported by AFOSR grant FA9550-18-1-0217 and NSF grant DMS1616954.

†Department of Mathematics, University of Michigan, Ann Arbor, MI 48109 (borcea@umich.edu).
‡Centre de Mathematiques Appliquees, Ecole Polytechnique, Palaiseau Cedex 91128, France (josselin.garnier@polytechnique.edu).
§Department of Mathematics, University of California, Irvine, CA 92697 (ksolna@math.uci.edu).

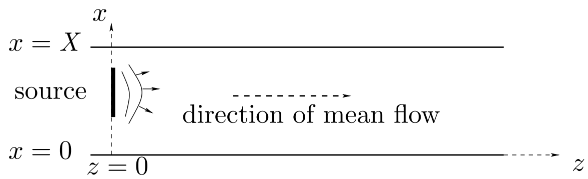

FIG. 1. *Illustration of the setup. A stationary source emits a wave in the range direction z in a waveguide filled with a moving random medium. The direction of the mean flow velocity $\langle \boldsymbol{v}(\boldsymbol{x})\rangle$ is along the range axis z. The system of coordinates is $\boldsymbol{x} = (x, z)$, with cross-range $x \in (0, X)$.*

amplitudes are random fields which describe mathematically the effect of scattering in the random waveguide. The mode coupling theory is developed in [2, 10, 13, 14, 15, 19] for waveguides filled with time-independent random media and in [3, 4, 5, 7, 16] for waveguides with random boundaries. In this paper we extend the theory to waveguides filled with time-dependent random media.

Time-dependent random waveguides arise in studies of sound propagation in the ocean, where the motion is due to currents, synoptic eddies, tides, and internal waves [24, section 1.3]. Typical relative sound speed fluctuation in the ocean are of the order of 10^{-3}–10^{-2}, and $|\boldsymbol{v}|/c_o$ is of the order of 10^{-3}. These are small variations, but they have a significant cumulative effect over a long range of propagation [11, 17, 18]. The estimation of oceanic flows using Doppler sonars is studied, for example, in [20, 27]. Other applications of waveguides with weakly turbulent flows are investigations of structural fatigue of flow duct systems in oil and gas industries [25], multiphase flow in pipes [29], monitoring drinking water quality in water distribution systems [1, 26], sound transmission through ventilation ducts [22], sound propagation through human airways for medical diagnosis [12], and design of musical instruments [9, 30].

In this paper we analyze, from first principles, sound propagation in a weakly turbulent flow in a two-dimensional waveguide $\mathcal{W} = \{\boldsymbol{x} = (x, z) \in (0, X) \times \mathbb{R}\}$ with diameter X. The restriction to two dimensions simplifies the analysis, but the results can be extended to three-dimensional waveguides. In waveguides with bounded cross-section (i.e., pipes), the extension may introduce mode degeneracy, meaning that multiple modes may share the same phase velocity. This degeneracy can be taken into account, using a similar analysis to that presented here, as illustrated, for example, in [2] for time-independent waveguides. In waveguides with unbounded cross-section, the guided modes are two-dimensional waves that propagate in the plane parallel to the boundary, as shown in [4], when the medium is stationary. The recent study [6] of wave propagation in moving random media would be relevant to understand their behavior and address this situation. The inverse problems we have in mind are, however, related to pipes, and that is why we focus our attention on this case.

Our analysis of the acoustic pressure $p(t, \boldsymbol{x})$ begins with the wave equation derived in [24, Chapter 2] via linearization of the equations of fluid dynamics about the flow with velocity $\boldsymbol{v}(t, \boldsymbol{x})$. This has small random fluctuations about the mean $\langle \boldsymbol{v}(\boldsymbol{x})\rangle$ with amplitude quantified by the dimensionless parameter ε satisfying $0 < \varepsilon \ll 1$. These fluctuations induce small and statistically correlated random fluctuations of the mass density and sound speed with ε-dependent amplitude. To analyze $p(t, \boldsymbol{x})$, we decompose it into propagating and evanescent modes with random amplitudes that satisfy a coupled system of stochastic differential equations driven by the fluctuations in the random medium. Then we use stochastic asymptotic analysis to characterize the statistics of the mode amplitudes in the limit $\varepsilon \to 0$. We study in particular the first two moments and show how to use them for estimating the mean flow velocity and locating a region of turbulent flow.

The paper is organized as follows: We begin in section 2 with the wave equation and model of the medium. Then we state in section 3 the results of the analysis of sound propagation in the random waveguide. Their derivation is in section 5. The inverse problems are in studied in section 4. We end with a summary in section 6.

2. Mathematical model. The wave equation for the acoustic pressure p is [24, equation (2.84)]

$$D_t\partial_t\left(\frac{D_t p(t,\boldsymbol{x})}{\rho(t,\boldsymbol{x})c^2(t,\boldsymbol{x})}\right) - \nabla_{\boldsymbol{x}}\cdot\partial_t\left(\frac{\nabla_{\boldsymbol{x}} p(t,\boldsymbol{x})}{\rho(t,\boldsymbol{x})}\right) + 2\sum_{i,j=1}^{2}\partial_{x_i}v_j(t,\boldsymbol{x})\partial_{x_j}\left(\frac{\partial_{x_i}p(t,\boldsymbol{x})}{\rho(t,\boldsymbol{x})}\right)$$

$$= -\frac{1}{\rho(t,\boldsymbol{x})}\nabla_{\boldsymbol{x}}\cdot\partial_t\boldsymbol{F}(t,\boldsymbol{x}), \qquad t\in\mathbb{R}, \quad \boldsymbol{x}\in\mathcal{W}, \tag{2.1}$$

where ∂_t is the partial derivative in t, $\nabla_{\boldsymbol{x}}$ is the gradient in $\boldsymbol{x}$, and $D_t = \partial_t + \boldsymbol{v}(t,\boldsymbol{x})\cdot\nabla_{\boldsymbol{x}}$ is the material (Lagrangian) derivative. The system of coordinates is $\boldsymbol{x} = (x_1, x_2)$ with cross-range $x_1 = x \in (0, X)$ and range $x_2 = z \in \mathbb{R}$ and $\boldsymbol{v} = (v_1, v_2)$.

Equation (2.1) is derived in [24, Chapter 2] from the linearization of the equations of fluid dynamics about a flow, followed by simplifications based on the assumption that $|\boldsymbol{v}| \ll c_o$ and the time variations of the flow are slow with respect to the period of oscillation of the sound wave generated by the source $\boldsymbol{F}$. The variable density ρ, sound speed c, and velocity $\boldsymbol{v}$ model the random medium and the flow. They satisfy the conservation of mass equation [24, equation (2.14)]

$$D_t \ln\rho(t,\boldsymbol{x}) + \nabla_{\boldsymbol{x}}\cdot\boldsymbol{v}(t,\boldsymbol{x}) = 0, \qquad t\in\mathbb{R}, \quad \boldsymbol{x}\in\mathcal{W}, \tag{2.2}$$

and the relation [24, equation (2.19)]

$$D_t c^2(t,\boldsymbol{x}) = \left(\frac{\partial^2 P(t,\boldsymbol{x})}{\partial\rho^2(t,\boldsymbol{x})}\right)_0 D_t\rho(t,\boldsymbol{x}), \qquad t\in\mathbb{R}, \quad \boldsymbol{x}\in\mathcal{W}, \tag{2.3}$$

where P is the reference pressure and the index 0 means that the derivative is evaluated in the reference state.

The analysis in [24] that establishes (2.1) is carried out in the whole space $\mathbb{R}^3$. Here we consider flow in the waveguide $\mathcal{W}$ (model of a pipe) that is filled with a random heterogeneous fluid and has sound hard walls,

$$\partial_x p(t,\boldsymbol{x}) = 0, \qquad t\in\mathbb{R}, \quad \boldsymbol{x}\in\partial\mathcal{W}, \tag{2.4}$$

where $\partial\mathcal{W} = \{0, X\}\times\mathbb{R}$. The flow velocity satisfies the no-slip condition

$$\boldsymbol{v}(t,\boldsymbol{x}) = \boldsymbol{0}, \qquad t\in\mathbb{R}, \quad \boldsymbol{x}\in\partial\mathcal{W}, \tag{2.5}$$

and the normal derivatives of the density and sound speed vanish at the walls,

$$\partial_x\rho(t,\boldsymbol{x}) = 0, \qquad \partial_x c(t,\boldsymbol{x}) = 0, \qquad t\in\mathbb{R}, \quad \boldsymbol{x}\in\partial\mathcal{W}. \tag{2.6}$$

The source $\boldsymbol{F}$ is compactly supported in space and time, and prior to the excitation there is no sound wave, so we have the initial condition

$$p(t,\boldsymbol{x}) \equiv 0, \qquad t \ll 0, \quad \boldsymbol{x}\in\mathcal{W}. \tag{2.7}$$

The no-slip condition (2.5) is typical for flow in pipes, and it arises either because of fluid viscosity or because of rough walls [28]. In the first case, one should add a viscous stress term in the equation of conservation of momentum in [24, Chapter 2] and note that if the viscosity is not too large, then it can be neglected in the linearized equations that lead to model (2.3). In the second case, there is no viscosity, but (2.5) is an effective boundary condition due to the interaction of the fluid with small-amplitude irregularities (corrugation) of the walls. For simplicity, in this paper we take flat walls, which means mathematically that we are in a scaling regime where the corrugation has small effect on the sound wave. However, the analysis can be extended to a corrugated boundary, using the techniques introduced in [3, 4, 16] for waveguides with random boundaries.

The motivation of our analysis comes from sound propagation in flows of heterogeneous fluids in pipes, which may become turbulent. As mentioned in the introduction, this is relevant, for instance, in the context of flow of water or oil and gas pipes [26, 1], and it motivates one of the inverse problems considered in section 4, which seeks to detect and localize a region of turbulent flow from measurements of the sound wave made at a remote location in the pipe.

2.1. Model of ideal flow. The unperturbed (ideal) flow is laminar, steady, and uniform, i.e., range independent. The medium has constant density ρ_o and sound speed c_o, and the flow velocity is of the form

$$\boldsymbol{v}(t,\boldsymbol{x}) = \langle \boldsymbol{v}(\boldsymbol{x})\rangle = \varepsilon V m_o(x)\boldsymbol{e}_z, \tag{2.8}$$

where $\boldsymbol{e}_z$ is the unit vector pointing in the range direction.

Note that (2.8) is independent of range and it is divergence free, consistent with (2.2). The transverse profile of $\boldsymbol{v}$ is modeled by the dimensionless function $m_o(x)$, which is typically a parabola that vanishes at $x \in \{0, X\}$ and reaches its maximum value 1 at $x = X/2$ [23, Chapter 8]. The dimensionless parameter ε used in the asymptotic analysis is defined so that $|\boldsymbol{v}|/c_o \sim \varepsilon \ll 1$, and $V \sim c_o$ is a normalized velocity scale. The symbol "$\sim$" denotes throughout equal, up to an $O(1)$ factor.

2.2. Model of the random flow. We consider small deviations from the ideal flow, where the mass density ρ and sound speed c are modeled by

$$\rho(t,\boldsymbol{x}) = \rho_o \exp\Big[\sqrt{\varepsilon}\mu_\rho\big(\varepsilon t, \boldsymbol{x}, \varepsilon z\big)\Big], \qquad c^{-2}(t,\boldsymbol{x}) = c_o^{-2}\Big[1 + \sqrt{\varepsilon}\mu_c\big(\varepsilon t, \boldsymbol{x}, \varepsilon z\big)\Big], \tag{2.9}$$

and the flow velocity $\boldsymbol{v}$ has mean $\langle \boldsymbol{v}\rangle$ that varies slowly in range,

$$\boldsymbol{v}(t,\boldsymbol{x}) = \varepsilon V\Big[m\big(x,\varepsilon z\big)\boldsymbol{e}_z + \sqrt{\varepsilon}\boldsymbol{\mu}_{\boldsymbol{v}}(\varepsilon t, \boldsymbol{x}, \varepsilon z)\Big], \qquad \langle \boldsymbol{v}(\boldsymbol{x})\rangle = \varepsilon V m\big(x, \varepsilon z\big)\boldsymbol{e}_z. \tag{2.10}$$

Here we recall that $\boldsymbol{x} = (x, z)$ and μ_ρ, μ_c, and $\boldsymbol{\mu}_{\boldsymbol{v}}$ are zero-mean, statistically correlated random processes. We assume that their relative amplitude is of the order $\sqrt{\varepsilon}$ because this is the scaling that produces a nontrivial interaction between the sound wave and the flow through (2.1). We will see that these small perturbations generate corrective terms in the wave propagation that become of order one after a propagation distance of order λ_o/ε, where λ_o is the central wavelength defined in the next section. We allow for a slow evolution of the flow at this long-range scale, hence the dependence in $T = \varepsilon t$ and $Z = \varepsilon z$ for the random processes.

The processes $\mu_\rho(T, x, z, Z)$, $\mu_c(T, x, z, Z)$, and $\boldsymbol{\mu}_{\boldsymbol{v}}(T, x, z, Z)$ are assumed statistically stationary in T and z. This means that the random fluctuations in (2.9)–(2.10) are locally stationary in range. Along the z-axis, the length scale of the fluctuations is of the order of λ_o, and the length scale of nonstationarity is of the order of λ_o/ε. This is captured by the Z-dependence of the random processes. The flow varies on the time scale of order T_o/ε, where T_o is the acoustic period defined in the next section, whereas the time scale of nonstationarity is larger than T_o/ε. Since the travel time to a range of order λ_o/ε is of order T_o/ε, we do not model these nonstationary temporal variations.

We also assume that $\mu_\rho(T,x,z,Z)$, $\mu_c(T,x,z,Z)$, and $\boldsymbol{\mu_v}(T,x,z,Z)$ are twice differentiable, with bounded derivatives almost surely, and have ergodic properties in z. We refer the reader to Appendix A for more details, which show that the model (2.9)–(2.10) is compatible with (2.2)–(2.3).

2.3. Model of the source. The source $\boldsymbol{F}$ in (2.1) is located at the origin of range. We model it as

$$\boldsymbol{F}(t,\boldsymbol{x}) = e^{-i\omega_o t} f\left(\frac{\varepsilon t}{T_f}, x\right)\delta(z)\boldsymbol{e}_z, \tag{2.11}$$

where ω_o is the central frequency that defines the central wavelength $\lambda_o = 2\pi/k_o$ and $k_o = \omega_o/c_o$ is the central wavenumber. The acoustic period is $T_o = 2\pi/\omega_o$. The function $f(\cdot,x)$ in (2.11) is the envelope of the oscillatory signal emitted by the source from the coordinate x in its cross-range support. The envelope varies slowly in time on the time scale T_f/ε that is of the order of the travel time of the waves to the range of order λ_o/ε, where $T_f \sim T_o$.

3. Statistics of the sound wave. The analysis in section 5 shows that if the correlation functions

$$\mathcal{R}_{cc}(\tau,x,x',\zeta,Z) = \mathbb{E}\left[\mu_c(\tau,x,\zeta,Z)\mu_c(0,x',0,Z)\right], \tag{3.1}$$

$$\mathcal{R}_{\rho\rho}(\tau,x,x',\zeta,Z) = \mathbb{E}\left[\mu_\rho(\tau,x,\zeta,Z)\mu_\rho(0,x',0,Z)\right], \tag{3.2}$$

$$\mathcal{R}_{c\rho}(\tau,x,x',\zeta,Z) = \mathbb{E}\left[\mu_c(\tau,x,\zeta,Z)\mu_\rho(0,x',0,Z)\right], \tag{3.3}$$

$$\mathcal{R}_{\rho c}(\tau,x,x',\zeta,Z) = \mathbb{E}\left[\mu_\rho(\tau,x,\zeta,Z)\mu_c(0,x',0,Z)\right] \tag{3.4}$$

are smooth enough in the range offset ζ, the acoustic pressure p at positive long-range $z = Z/\varepsilon$ and commensurate time $t = T/\varepsilon$ is given by

$$p\left(\frac{T}{\varepsilon}, x, \frac{Z}{\varepsilon}\right) \approx \sum_{j=0}^{N} \phi_j(x)\exp\left[i\frac{(\beta_j Z - \omega_o T)}{\varepsilon}\right]\pi_j^\varepsilon(T,Z). \tag{3.5}$$

The terms in this sum are defined by

$$\pi_j^\varepsilon(T,Z) = \int_{-\infty}^{\infty}\frac{d\omega}{2\pi}\,\widehat{\pi}_j^\varepsilon(\omega,Z)e^{-i\omega T}, \qquad \widehat{\pi}_j^\varepsilon(\omega,Z) = \frac{a_j^\varepsilon(\omega,Z)}{\sqrt{\beta_j}}e^{i\omega\beta_j' Z}, \tag{3.6}$$

and

$$\phi_j(x) = \sqrt{\frac{2-\delta_{j0}}{X}}\cos\left(\frac{\pi j x}{X}\right), \qquad j \geq 0, \tag{3.7}$$

where δ_{j0} is the Kronecker delta symbol and

$$\beta_j = \sqrt{k_o^2 - \left(\frac{\pi j}{X}\right)^2}, \qquad \beta_j' = \frac{k_o}{c_o\beta_j}, \qquad j = 0,\dots,N = \lfloor k_o X/\pi\rfloor, \tag{3.8}$$

with $\lfloor\cdot\rfloor$ denoting the integer part.

The expression (3.5) is a superposition of $N+1$ time-harmonic plane waves with frequency $\omega_o + \varepsilon\omega$ and wave vectors

$$\boldsymbol{K}_j^{\pm} = \left(\pm \frac{\pi j}{X}, \beta_j + \varepsilon \omega \beta_j' \right), \qquad j = 0, \dots, N. \tag{3.9}$$

They define the propagating modes $\pi_j^\varepsilon(T,Z) \exp[i(\beta_j Z - \omega_o T)/\varepsilon]$, which are one-dimensional forward-going waves with wavenumber β_j and group speed $1/\beta_j'$. The amplitudes a_j^ε of these waves are random fields, which model the long-range cumulative effect of scattering in the random waveguide.

We show in section 5.3.2 that in the limit $\varepsilon \to 0$, the mode amplitudes can be characterized by a Markov process $\{a_j(\omega, Z)\}_{\omega \in \mathbb{R}, 0 \le j \le N}$ as follows: For any Schwartz test function $\widehat{\varphi}(\omega)$, we have

$$\int_{-\infty}^{\infty} d\omega\, \widehat{\varphi}(\omega) a_j^\varepsilon(\omega, Z) \xrightarrow{\varepsilon \to 0} \int_{-\infty}^{\infty} d\omega\, \widehat{\varphi}(\omega) a_j(\omega, Z), \qquad j = 0, \dots, N, \tag{3.10}$$

where the limit is in distribution. The approximation in (3.5) is in this weak limit, meaning that

$$\varphi(T) \star_T \pi_j^\varepsilon(T, Z) \xrightarrow{\varepsilon \to 0} \int_{-\infty}^{\infty} \frac{d\omega}{2\pi}\, \widehat{\varphi}(\omega) \frac{a_j(\omega, Z)}{\sqrt{\beta_j}} e^{i\omega(\beta_j' Z - T)}, \tag{3.11}$$

in distribution, for $j = 0, \dots, N$ and for any Schwartz test function $\widehat{\varphi}$, with inverse Fourier transform φ. The symbol $\star_T$ denotes convolution in T.

One can calculate all the statistical moments of the limit mode amplitudes using the infinitesimal generator of the Markov process $\{a_j(\omega, Z)\}_{\omega \in \mathbb{R}, 0 \le j \le N}$ given in section 5.3.2. Here we describe the first two moments, which are used to solve the inverse problems in section 4.

3.1. Coherent wave. The expectation of the pressure field, called the "coherent wave," is obtained from (3.5) and (3.11) using the mean mode amplitudes

$$\mathbb{E}[a_j(\omega, Z)] = a_{j,o}(\omega) \exp\left\{ -i\Phi_j(Z) + \int_0^Z dZ' \left[\Theta_j(Z') + i\Psi_j(Z')\right] \right\}. \tag{3.12}$$

These differ from the amplitudes $a_{j,o}$ in the ideal waveguide, without flow,

$$a_{j,o}(\omega) = \frac{\sqrt{\beta_j} T_f}{2} \widehat{f}_j(\omega T_f), \qquad \widehat{f}_j(\omega T_f) = \int_{-\infty}^{\infty} ds\, e^{i\omega T_f s} \int_0^X dx\, f(s,x) \phi_j(x), \tag{3.13}$$

by the exponential in (3.12). The first term in the exponent is the phase

$$\Phi_j(Z) = \frac{V}{c_o} \int_0^Z dZ'\, M_{jj}(Z') \tag{3.14}$$

due to the mean flow, where

$$\begin{aligned} M_{jj}(Z) = {} & \delta_{j0} k_o \int_0^X \frac{dx}{X}\, m(x,Z) \\ & + (1 - \delta_{j0}) \left\{ k_o \int_0^X \frac{dx}{X}\, m(x,Z) \right. \\ & \left. + \left[k_o - \frac{2}{k_o} \left(\frac{\pi j}{X} \right)^2 \right] \int_0^X \frac{dx}{X}\, m(x,Z) \cos\left(\frac{2\pi j x}{X} \right) \right\}. \end{aligned} \tag{3.15}$$

The other two terms are due to the random medium,

$$\Theta_j(Z) = -\sum_{l=0}^{N} \frac{1}{4\beta_l\beta_j} \int_0^\infty d\zeta\, e^{i(\beta_l-\beta_j)\zeta} \mathcal{C}_{j,l,j,l}(0,\zeta,Z), \tag{3.16}$$

$$\Psi_j(Z) = \frac{1}{2\beta_j}\int_0^X dx\, \phi_j^2(x)(\partial^2_{xx'} - \partial^2_\zeta)\mathcal{R}_{\rho\rho}(0,x,x',\zeta,Z)\,|_{x'=x,\zeta=0}$$
$$+ \sum_{l=N+1}^{\infty} \frac{1}{4\beta_l\beta_j}\int_{-\infty}^{\infty} d\zeta e^{-\beta_l|\zeta|}\cos(\beta_j\zeta)\mathcal{C}_{j,l,j,l}(0,\zeta,Z). \tag{3.17}$$

They are defined by the correlation function $\mathcal{R}_{\rho\rho}$ and by

$$\mathcal{C}_{j,l,j,l}(\tau,\zeta,Z) = \mathbb{E}\Big[\Gamma_{j,l}(0,0,Z)\Gamma_{j,l}(\tau,\zeta,Z)\Big], \tag{3.18}$$

the correlation function of the random process

$$\Gamma_{j,l}(\tau,\zeta,Z) = \int_0^X dx\, \phi_j(x)\phi_l(x)\left[k_o^2\mu_c(\tau,x,\zeta,Z) + \frac{1}{2}\Delta_{(x,\zeta)}\mu_\rho(\tau,x,\zeta,Z)\right], \tag{3.19}$$

which is stationary in τ and ζ. Here $\Delta_{(x,\zeta)} = \partial_x^2 + \partial_\zeta^2$ is the Laplacian operator.

Remark 3.1. Equation (3.12) and definition (3.16) give that

$$\big|\mathbb{E}[a_j(\omega,Z)]\big| = \big|a_{j,o}(\omega)\big|\exp\left[-\int_0^Z dZ' \sum_{l=0}^{N} \frac{1}{16\pi\beta_l\beta_j}\int_{-\infty}^{\infty} d\omega\, \widehat{\mathcal{C}}_{j,l,j,l}(\omega,\beta_l-\beta_j,Z')\right],$$

where by Bochner's theorem

$$\widehat{\mathcal{C}}_{j,l,j,l}(\omega,\beta_l-\beta_j,Z) = \int_{-\infty}^{\infty} d\tau\, e^{i\omega\tau}\int_{-\infty}^{\infty} d\zeta\, e^{i(\beta_l-\beta_j)\zeta}\mathcal{C}_{j,l,j,l}(\tau,\zeta,Z) \geq 0. \tag{3.20}$$

Thus, the mean amplitudes decay with Z at a mode-dependent rate. This decay models the randomization (loss of coherence) of the wave.

Remark 3.2. Equations (3.12)–(3.15) show that the mean flow affects only the phases (3.14) of the mean mode amplitudes. As shown in Appendix A, the random fluctuations μ_ρ and μ_c are affected by the mean flow (see (A.1)–(A.2)), but the statistical quantities $\mathcal{C}_{j,l}$ are independent of the mean flow.

Remark 3.3. It seems that the evanescent component of p has been neglected in (3.5). However, this component plays a role because scattering in the random medium couples the propagating and evanescent modes. This coupling is taken into account in the analysis in section 5, and its net effect is in the second term of the phase (3.17).

Remark 3.4. Only the fluctuations μ_c and μ_ρ of the wave speed and density enter the expressions of the effective coefficients (3.16)–(3.17). The analysis in section 5 shows that the terms in the wave equation that involve the velocity fluctuations $\boldsymbol{\mu_v}$ vanish in the limit $\varepsilon \to 0$. Nevertheless, incorporating these fluctuations is important for the consistency of the modeling, as explained in Appendix A.

3.2. Transport of energy. Consider the analogue of (3.6) for the limit amplitudes

$$\pi_j(T,Z) = \int_{-\infty}^{\infty} \frac{d\omega}{2\pi}\, \widehat{\pi}_j(\omega,Z)e^{-i\omega T}, \qquad \widehat{\pi}_j(\omega,Z) = \frac{a_j(\omega,Z)}{\sqrt{\beta_j}}e^{i\omega\beta_j' Z}. \tag{3.21}$$

This is the jth propagating mode in the weak limit $\varepsilon \to 0$ described in (3.11), corresponding to the superposition of the plane waves with wave vectors (3.9). The energy density of these waves is defined by the mode-dependent mean Wigner transform

$$
\begin{aligned}
W_j(\omega,\tau,Z) &= \beta_j \int_{-\infty}^{\infty} dT\, \mathbb{E}\Big[\pi_j\Big(\tau+\frac{T}{2},Z\Big)\overline{\pi_j\Big(\tau-\frac{T}{2},Z\Big)}\Big]e^{i\omega T} \\
&= \int_{-\infty}^{\infty}\frac{dw}{2\pi}\,\mathbb{E}\Big[a_j\Big(\omega+\frac{w}{2},Z\Big)\overline{a_j\Big(\omega-\frac{w}{2},Z\Big)}\Big]e^{iw(\beta_j' Z-\tau)}, \qquad (3.22)
\end{aligned}
$$

where the bar denotes throughout complex conjugate.

The mean Wigner transform satisfies the system of transport equations

$$
\begin{aligned}
\big(\partial_Z+\beta_j'\partial_\tau\big)W_j(\omega,\tau,Z) = \sum_{l=0}^{N}\frac{1}{8\pi\beta_j\beta_l}\int_{-\infty}^{\infty} & d\omega'\,\widehat{\mathcal{C}}_{l,j,l,j}(\omega',\beta_j-\beta_l,Z) \\
&\times\big[W_l(\omega-\omega',\tau,Z)-W_j(\omega,\tau,Z)\big] \qquad (3.23)
\end{aligned}
$$

at $Z>0$ with initial condition

$$
W_j(\omega,\tau,0)=W_{j,o}(\omega,\tau)=\int_{-\infty}^{\infty}\frac{dw}{2\pi}\,a_{j,o}\Big(\omega+\frac{w}{2}\Big)\overline{a_{j,o}\Big(\omega-\frac{w}{2}\Big)}e^{-iw\tau} \qquad (3.24)
$$

for $j=0,\ldots,N$. The integral kernel in these equations determines the energy exchange among the modes. It satisfies

$$
\frac{1}{2}\sum_{l=0}^{N}\frac{1}{8\pi\beta_j\beta_l}\int_{-\infty}^{\infty}d\omega'\,\widehat{\mathcal{C}}_{l,j,l,j}(\omega',\beta_j-\beta_l,Z) = -\mathrm{Re}\big[\Theta_j(Z)\big], \qquad (3.25)
$$

where the right-hand side is the inverse of the range scale of decay of the mean mode amplitudes (3.12). By definitions (3.18)–(3.19) and (3.20), we also have the symmetry relations

$$
\widehat{\mathcal{C}}_{l,j,l,j}(\omega,\beta_j-\beta_l,Z)=\widehat{\mathcal{C}}_{j,l,j,l}(\omega,\beta_l-\beta_j,Z),
$$

which imply from (3.22) that

$$
\partial_Z\sum_{j=0}^{N}\int_{-\infty}^{\infty}d\omega\int_{-\infty}^{\infty}d\tau\,W_j(\omega,\tau,Z)=\partial_Z\int_{-\infty}^{\infty}d\omega\sum_{j=0}^{N}\mathbb{E}\Big[\big|a_j(\omega,Z)\big|^2\Big]=0. \qquad (3.26)
$$

This shows that the mean energy stored in the propagating modes is conserved in the limit $\varepsilon\to 0$.

4. Inverse problems.

We now use the theory summarized in section 3 to estimate the flow from measurements of the pressure at an array of receivers at range $z_{\mathcal{A}}=Z_{\mathcal{A}}/\varepsilon$ and cross-range in the interval (array aperture) $\mathcal{A}\subseteq(0,X)$. The receivers should record for time $t\geq O(T_o/\varepsilon)$ to capture the arrival of at least some modes. To simplify the mathematical expressions, we take an infinite time recording window.

4.1. Estimation of mean flow.

The mean flow velocity $\langle \boldsymbol{v}\rangle$ does not affect the transport of energy in the waveguide, but it appears in the phase (3.14) of the mode amplitudes (3.12) of the coherent wave.

To estimate this phase from the array measurements, calculate

$$\mathcal{P}_j\left(\frac{T}{\varepsilon}\right) = \int_{\mathcal{A}} dx\, \phi_j(x) p\left(\frac{T}{\varepsilon}, x, \frac{Z_{\mathcal{A}}}{\varepsilon}\right), \tag{4.1}$$

and obtain from (3.5) that

$$\mathcal{P}_j\left(\frac{T}{\varepsilon}\right) \approx \sum_{l=1}^{N} C^{\mathcal{A}}_{j,l} \exp\left[i\frac{(\beta_l Z_{\mathcal{A}} - \omega_o T)}{\varepsilon}\right] \pi^{\varepsilon}_l(T, Z_{\mathcal{A}}), \tag{4.2}$$

where we introduced the $(N+1)\times(N+1)$ coupling matrix $\boldsymbol{C}^{\mathcal{A}}$ with entries

$$C^{\mathcal{A}}_{j,l} = \int_{\mathcal{A}} dx\, \phi_j(x)\phi_l(x). \tag{4.3}$$

When the array has full aperture, this matrix equals the identity. We allow for a smaller aperture of length $|\mathcal{A}| < X$ but suppose that $|\mathcal{A}|/X$ is not too small so that $\boldsymbol{C}^{\mathcal{A}}$ is invertible [31]. Then we obtain from (4.1), with $\boldsymbol{\mathcal{P}} = (\mathcal{P}_0, \dots, \mathcal{P}_N)^T$, that

$$\left[(\boldsymbol{C}^{\mathcal{A}})^{-1}\boldsymbol{\mathcal{P}}\left(\frac{T}{\varepsilon}\right)\right]_j \approx \exp\left[i\frac{(\beta_j Z_{\mathcal{A}} - \omega_o T)}{\varepsilon}\right] \pi^{\varepsilon}_j(T, Z_{\mathcal{A}}). \tag{4.4}$$

We are interested in the coherent part of (4.4), which can be approximated in the weak limit $\varepsilon \to 0$, as explained in section 3.1. Inverting the exponential in (4.4), smoothing by convolution with a Schwartz test function φ, using (3.11), taking expectation, and substituting the mean amplitudes (3.12), we get

$$\begin{aligned}
&\exp\left[-i\frac{(\beta_j Z_{\mathcal{A}} - \omega_o T)}{\varepsilon}\right] \int_{-\infty}^{\infty} dT' \varphi(T') e^{-i\omega_o t'} \mathbb{E}\left[\left[(\boldsymbol{C}^{\mathcal{A}})^{-1}\boldsymbol{\mathcal{P}}\Big(\frac{T-T'}{\varepsilon}\Big)\right]_j\right] \\
&\approx \frac{1}{2}\int_{-\infty}^{\infty} dT' \varphi(T') f_j\left(\frac{T - T' - \beta_j' Z_{\mathcal{A}}}{T_f}\right) \\
&\times \exp\left\{-i\Phi_j(Z_{\mathcal{A}}) + \int_0^{Z_{\mathcal{A}}} dZ\, \left[\Theta_j(Z) + i\Psi_j(Z)\right]\right\},
\end{aligned} \tag{4.5}$$

where f_j is the inverse Fourier transform of $\widehat{f}_j$ defined in (3.13).

This equation holds for any test function, so we can choose $\varphi(T)$ to be negligible outside an interval $[-T_\varphi, T_\varphi] \subset [-T_f, T_f]$ with $T_\varphi \ll T_f$. Then the right-hand side of (4.5) peaks at $T \approx \beta_j' Z_{\mathcal{A}}$ or, in unscaled variables, at time $t \approx t_j = \beta_j' z_{\mathcal{A}}$. We can interpret it as the source signal arriving at travel time t_j, damped and with an extra phase due to the mean flow and random medium. If the effect of the random medium is not too strong, meaning that the last term in the exponential in (4.5) is small, the approximation holds even without expectation, so we can estimate $\Phi_j(Z_{\mathcal{A}})$.

Remark 4.1. The statistical stability of the estimate of $\Phi_j(Z_{\mathcal{A}})$ can be enhanced by considering several well-separated pulses and averaging the results.

We infer from definitions (3.15) and (3.14) that $|\Phi_j(Z_{\mathcal{A}})| \sim k_o Z_{\mathcal{A}} V/c_o$, and definitions (3.16)–(3.17) and (3.18)–(3.19) give that

$$\begin{aligned}\big|\Theta_j(Z)\big| &\sim \frac{1}{k_o^2\sqrt{1-(j/N)^2}} \sum_{l=0}^{N} \frac{1}{\sqrt{1-(l/N)^2}} \left| \int_0^\infty d\zeta \, e^{i(\beta_l-\beta_j)\zeta} \mathcal{C}_{j,l,j,l}(0,\zeta,Z) \right| \\ &\sim \frac{k_o^2 \sigma_c^2 \ell N}{\sqrt{1-(j/N)^2}} \frac{1}{N} \sum_{l=0}^{N} \frac{1}{\sqrt{1-(l/N)^2}} \\ &\sim \frac{k_o^3 \sigma_c^2 \ell X}{\sqrt{1-(j/N)^2}}\end{aligned}$$

and similar for $\Psi_j(Z)$. Here we used (3.8) and introduced the standard deviation σ_c and the correlation length ℓ in the range direction of the random fluctuations of the sound speed and density, which gives the order of magnitude of the ζ integral in the first line. We also used that $k_o \sim 1/X$. These estimates show that Φ_j dominates the other terms in the exponential in the right-hand side of (4.5) if

$$|\Phi_j(Z_{\mathcal{A}})| \gg \left| \int_0^{Z_{\mathcal{A}}} dZ \left[\Theta_j(Z) + i\Psi_j(Z)\right] \right|, \quad \text{i.e., if} \quad \frac{V}{c_o} \gg \frac{k_o^2 \sigma_c^2 \ell X}{\sqrt{1-(j/N)^2}}. \tag{4.6}$$

The bound in this equation grows with j, showing that it is difficult to estimate Φ_j for the higher-order modes, whose mean amplitudes are strongly damped at $z_{\mathcal{A}} = Z_{\mathcal{A}}/\varepsilon$.

Assuming that (4.6) holds for $j \le J \le N$, we now explain how to extract information about the mean flow from $\{\Phi_j(Z_{\mathcal{A}})\}_{0\le j\le J}$. Since the functions (3.5) form an $L^2([0,X])$ basis $\{\phi_j(x)\}_{j\ge 0}$, let us expand the mean velocity profile in this basis:

$$m(x,Z) = \sum_{j=0}^{\infty} m_j(Z)\phi_j(x). \tag{4.7}$$

Definitions (3.14)–(3.15) show that from Φ_j we can determine the following range-integrated, even-indexed coefficients in this expansion:

$$\int_0^{Z_{\mathcal{A}}} dZ \, m_{2j}(Z) = \int_0^{Z_{\mathcal{A}}} dZ \int_0^X dx \, \phi_{2j}(x) m(x,Z), \qquad 0 \le j \le J/2. \tag{4.8}$$

This is not enough information to reconstruct $m(x,Z)$, but it can determine whether the mean flow is laminar, with the parabolic profile $m_{\rm lam}(x) = 4x/X(1-x/X)$ [23, Chapter 8], or whether there are range variations of the mean flow velocity.

Remark 4.2. The phases $\{\Phi_j(Z_{\mathcal{A}})\}_{0\le j\le J}$ can be estimated only modulo 2π. The modulo 2π ambiguity can be avoided at low frequency, where

$$\Phi_j(Z_{\mathcal{A}}) \sim k_o Z_{\mathcal{A}} V/c_o < 2\pi, \qquad j = 0, \ldots, J. \tag{4.9}$$

Having a low frequency is also beneficial in (4.6).

Remark 4.3. If condition (4.9) does not hold, but m varies from the laminar profile $m_{\rm lam}$ in a small range interval ΔL, then it is feasible to detect this variation from the phases if $k_o \Delta L V/c_o < 2\pi$.

4.2. Localization of a region of turbulent flow. We describe here how to use the transport theory summarized in section 3.2 for detecting and localizing a region of turbulent flow in the interval $Z \in (L, L+\Delta L)$ on the left side of the receiver array, as illustrated in Figure 2. We begin with the explicit expression of the mean Wigner transform and then show how to use it for the inverse problem.

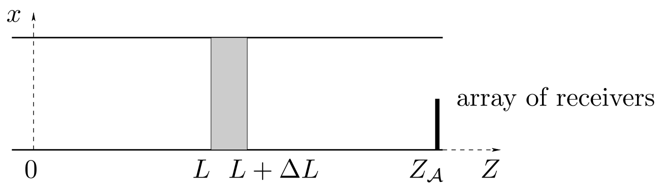

FIG. 2. *Illustration of the setup for localizing a region of turbulent flow in the scaled range interval* $Z \in (L, L+\Delta L)$ *using measurements at an array of receivers at scaled range* $Z_{\mathcal{A}}$.

4.2.1. Mean Wigner transform. The flow is ideal at $Z \notin (L, L+\Delta L)$, so we can write

$$W_j(\omega,\tau,Z_{\mathcal{A}}) = W_j\big(\omega, \tau - \beta_j'(Z_{\mathcal{A}} - L - \Delta L), L+\Delta L\big), \qquad j = 0,\ldots,N, \tag{4.10}$$

where the right-hand side is the mean Wigner transform at scaled range $L+\Delta L$. It satisfies (3.23) at $Z \in (L, L+\Delta L)$ with initial condition defined in (3.24):

$$W_j(\omega,\tau,L) = W_{j,o}(\omega, \tau - \beta_j' L), \qquad j = 0,\ldots,N. \tag{4.11}$$

Using Fourier transforms to deal with the convolution in ω and the τ derivative in (3.23), we obtain that

$$W_j(\omega,\tau,L+\Delta L) = \int_{-\infty}^{\infty} d\omega' \int_{-\infty}^{\infty} d\tau' \sum_{l=0}^{N} S_{j,l}(\omega',\tau') W_l(\omega-\omega', \tau-\tau', L) \tag{4.12}$$

with coupling matrix $\boldsymbol{S} = (S_{j,l})_{0\le j,l\le N}$ defined by

$$\boldsymbol{S}(\omega,\tau) = \frac{1}{4\pi^2}\int_{-\infty}^{\infty} dt\, e^{i\omega t}\int_{-\infty}^{\infty} dw\, e^{-iw\tau}\mathfrak{S}(L+\Delta L; t, w). \tag{4.13}$$

Here $\mathfrak{S}$ is the state-transition matrix of the linear system

$$\begin{aligned} \partial_Z \mathfrak{S}(Z;t,w) &= \boldsymbol{\Upsilon}(Z;t,w)\mathfrak{S}(Z;t,w,L), \qquad Z > L,\\ \mathfrak{S}(L;t,w) &= \boldsymbol{I}_{N+1}, \end{aligned}$$

parametrized by t and w, where $\boldsymbol{I}_{N+1}$ is the $(N+1)\times(N+1)$ identity matrix and $\boldsymbol{\Upsilon} = (\Upsilon_{j,l})_{0\le j,l\le N}$ is the matrix with entries

$$\Upsilon_{j,l}(Z;t,w) = \Big(iw\beta_j' + 2\mathrm{Re}[\Theta_j(Z)]\Big)\delta_{jl} + \frac{1}{8\pi\beta_j\beta_l}\int_{-\infty}^{\infty} d\omega\, e^{-i\omega t}\widehat{\mathcal{C}}_{j,l,j,l}(\omega, \beta_j - \beta_l, Z).$$

The expression of the mean Wigner transform is obtained by substituting (4.11)–(4.12) in (4.10):

$$\begin{aligned} W_j(\omega,\tau,Z_{\mathcal{A}}) = \int_{-\infty}^{\infty} d\omega' \int_{-\infty}^{\infty} d\tau' \sum_{l=0}^{N} S_{j,l}(\omega',\tau') \\ \times W_{l,o}(\omega-\omega', \tau-\tau' - \beta_l' L - \beta_j'(Z_{\mathcal{A}} - L - \Delta L)), \quad j = 0,\ldots,N. \end{aligned} \tag{4.14}$$

We cannot write it more explicitly because the state-transition matrix does not have a closed-form expression. However, for a thin turbulent layer, with ΔL satisfying

$$\sup_{t,w\in\mathbb{R}} \int_L^{L+\Delta L} dZ\, \|\boldsymbol{\Upsilon}(Z;t,w)\|_2 < \pi,$$

the matrix $\mathfrak{S}$ has the Magnus expansion [21]

$$\mathfrak{S}(Z;t,w) = e^{\int_L^{L+\Delta L} dZ \left\{ \boldsymbol{\Upsilon}(Z;t,w) + \int_L^{L+\Delta L} dZ' \left[\boldsymbol{\Upsilon}(Z;t,w), \boldsymbol{\Upsilon}(Z';t,w) \right] + \cdots \right\}}, \tag{4.15}$$

where $[\cdot,\cdot]$ is the matrix commutator. Furthermore, since $\boldsymbol{\Upsilon}(Z;t,w)$ is continuously differentiable in Z, we can approximate $\mathfrak{S}$ by keeping only the first term in the expansion if ΔL is sufficiently small.

4.2.2. Estimation of the Wigner transform. We cannot obtain the mean Wigner transform (4.14) directly from the array data because its expression involves the weak limit $\varepsilon \to 0$ and the expectation. Here we explain how to estimate it from the jth mode $\pi_j^\varepsilon(T, Z_{\mathcal{A}})$ calculated as in (4.4).

Equations (3.11) and (3.21) give that for any Schwartz test function $\varphi(T)$, which we assume supported at $|T| \ll T_f$, we have

$$\varphi(T) \star_T \pi_j^\varepsilon(T, Z_{\mathcal{A}}) \overset{\varepsilon \to 0}{\longrightarrow} \varphi(T) \star_T \pi_j(T, Z_{\mathcal{A}}). \tag{4.16}$$

Denote by $\pi_j^{\varphi,\varepsilon}$ the convolution of π_j^ε and φ, the left-hand side in (4.16), and similarly, by π_j^φ the convolution of the limit π_j and φ. Then

$$\mathscr{W}_j^{\varphi,\varepsilon}(\omega,\tau,Z_{\mathcal{A}}) = \beta_j \int_{-\infty}^{\infty} dT\, \pi_j^{\varphi,\varepsilon}\left(\tau + \frac{T}{2}, Z_{\mathcal{A}}\right) \overline{\pi_j^{\varphi,\varepsilon}\left(\tau - \frac{T}{2}, Z_{\mathcal{A}}\right)} e^{i\omega T} \tag{4.17}$$

tends in the limit $\varepsilon \to 0$, in distribution, to

$$\begin{aligned} \mathscr{W}_j^{\varphi}(\omega,\tau,Z_{\mathcal{A}}) &= \beta_j \int_{-\infty}^{\infty} dT\, \pi_j^{\varphi}\left(\tau + \frac{T}{2}, Z_{\mathcal{A}}\right) \overline{\pi_j^{\varphi}\left(\tau - \frac{T}{2}, Z_{\mathcal{A}}\right)} e^{i\omega T} \\ &= \mathscr{W}^{\varphi}(\omega,\tau) \star_\tau \mathscr{W}_j(\omega,\tau,Z_{\mathcal{A}}), \end{aligned} \tag{4.18}$$

where

$$\mathscr{W}^{\varphi}(\omega,\tau) = \int_{-\infty}^{\infty} dT\, \varphi\left(\tau + \frac{T}{2}\right) \overline{\varphi\left(\tau - \frac{T}{2}\right)} e^{i\omega T} \tag{4.19}$$

is the Wigner transform of φ and

$$\mathscr{W}_j(\omega,\tau,Z_{\mathcal{A}}) = \beta_j \int_{-\infty}^{\infty} dT\, \pi_j\left(\tau + \frac{T}{2}, Z_{\mathcal{A}}\right) \overline{\pi_j\left(\tau - \frac{T}{2}, Z_{\mathcal{A}}\right)} e^{i\omega T}. \tag{4.20}$$

The expectation of (4.20) is the mean Wigner transform (3.22), and (4.14) and (4.17) give the following estimate of its convolution with (4.19):

$$\mathbb{E}[\mathscr{W}_j^{\varphi,\varepsilon}(\omega,\tau,Z_{\mathcal{A}})] \approx W_j^{\varphi}(\omega,\tau,Z_{\mathcal{A}}),$$

where

$$\begin{aligned} W_j^{\varphi}(\omega,\tau,Z_{\mathcal{A}}) := \mathscr{W}^{\varphi}(\omega,\tau) \star_\tau \int_{-\infty}^{\infty} d\omega' \int_{-\infty}^{\infty} d\tau' \sum_{l=0}^{N} S_{j,l}(\omega',\tau') \\ \times W_{l,o}(\omega-\omega', \tau-\tau'-\beta_l' L - \beta_j'(Z_{\mathcal{A}} - L - \Delta L)). \end{aligned} \tag{4.21}$$

4.2.3. Inversion. Suppose that the source excites only the $j_\star$th mode, and obtain from definitions (3.13) and (3.24) that

$$W_{j,o}(\omega,\tau) = \frac{\beta_{j_\star}\delta_{jj_\star}}{4} \int_{-\infty}^{\infty} dT\, f_{j_\star}\left(\frac{\tau + T/2}{T_f}\right) \overline{f_{j_\star}\left(\frac{\tau - T/2}{T_f}\right)} e^{i\omega T}. \tag{4.22}$$

Then the expression (4.21) becomes

$$
\begin{aligned}
W_j^{\varphi}(\omega,\tau,Z_{\mathcal{A}}) = \mathscr{W}^{\varphi}(\omega,\tau) \star_\tau \int_{-\infty}^{\infty} d\omega' \int_{-\infty}^{\infty} d\tau' S_{j,j_\star}(\omega',\tau') \\
\times W_{j_\star,o}(\omega-\omega',\tau-\tau'-T_j(L)+\beta_j'\Delta L),
\end{aligned} \tag{4.23}
$$

where we introduced the travel times $T_j(L) = \beta_{j_\star}' L + \beta_j'(Z_{\mathcal{A}} - L)$ for $j = 0,\dots,N$.

Note from (4.22) that $W_{j_\star,o}(\omega,\tau)$ peaks at $\tau = 0$ and is supported at $|\tau| \lesssim T_f$. Since the support of $\varphi(T)$ is at $|T| \ll T_f$, its Wigner transform (4.19) is supported at $|\tau| \ll T_f$. Therefore, the expression in (4.23) peaks at $\tau \approx T_j(L) - \beta_j'\Delta L + O(T_S)$, where T_S is the support in τ of the coupling matrix (4.13). Assuming that the layer of turbulence is thin, so that $\Delta L \ll Z_{\mathcal{A}} - L$, we have

$$
\beta_j'\Delta L \ll \beta_{j_\star}' L + \beta_j'(Z_{\mathcal{A}} - L) = T_j(L). \tag{4.24}
$$

Equations (4.13)–(4.15) also imply that T_S is small, when ΔL is small, so the peak of (4.23) is at $\tau \approx T_j(L)$. Then we can determine the range L by solving the minimization problem

$$
\widehat{L} = \underset{L_s\in(0,Z_{\mathcal{A}})}{\operatorname{argmin}} \sum_{j=0,j\neq j_\star}^{N_t} \int_{-\infty}^{\infty} d\omega \int_{-\infty}^{\infty} d\tau \big|W_j^{\varphi}(\omega,\tau,Z_{\mathcal{A}})\big|^2 \Big[1 - e^{-\left(\tau - T_j(L_s)\right)^2/T_f^2}\Big]. \tag{4.25}
$$

Remark 4.4. The turbulent flow causes transfer of energy from the initially excited $j_\star$th mode to the other modes. Therefore, its presence can be detected by calculating (4.17) from the array measurements. If this is large for $j \neq j_\star$, then a region of turbulent flow exists in the waveguide.

Remark 4.5. We described the estimation of L based on the expression (4.21). In practice we can only compute $\mathscr{W}_j^{\varphi,\varepsilon}$, not its expectation. Thus, W_j^{φ} in (4.25) is replaced by the random $\mathscr{W}_j^{\varphi,\varepsilon}$. This can still be modeled by an expression of the form (4.23) with random coupling matrix $\boldsymbol{S}^{\varepsilon}(\omega,\tau)$. As long as assumption (4.24) holds, the coupling gives a negligible travel time correction, so the minimizer is $\widehat{L} \approx L$.

5. Analysis of sound propagation. Here we derive the results stated in section 3. We begin in section 5.1 with the scaling. The mode decomposition is in section 5.2, and the analysis of the mode amplitudes is in section 5.3.

5.1. Long-range scaling. We are interested in the propagation of the sound wave at long-range z of order λ_o/ε and therefore for travel times of order T_o/ε. Thus, we introduce the scaled range and time

$$
Z = \varepsilon z, \quad T = \varepsilon t, \tag{5.1}
$$

where $Z \sim \lambda_o$ and $T \sim T_o$. We also define the field

$$
p^{\varepsilon}(T,x,Z) = \exp\left[-\frac{\sqrt{\varepsilon}}{2}\mu_\rho\left(T,x,\frac{Z}{\varepsilon},Z\right)\right] p\left(\frac{T}{\varepsilon},x,\frac{Z}{\varepsilon}\right), \tag{5.2}
$$

which differs from the acoustic pressure p by a factor $1+O(\sqrt{\varepsilon})$. Substituting in (2.1) and multiplying by ρ_o, we obtain

$$
\begin{aligned}
&\partial_{\frac{T}{\varepsilon}}\left(\frac{1}{c_o^2}\partial^2_{\frac{T}{\varepsilon}} - \Delta_{(x,\frac{Z}{\varepsilon})}\right)p^\varepsilon(T,x,Z)\\
&\quad+\sqrt{\varepsilon}\left[\frac{\mu_c\left(T,x,\frac{Z}{\varepsilon},Z\right)}{c_o^2}\partial^3_{\frac{T}{\varepsilon}} - \frac{1}{2}\Delta_{(x,\frac{Z}{\varepsilon})}\mu_\rho\left(T,x,\frac{Z}{\varepsilon},Z\right)\partial_{\frac{T}{\varepsilon}}\right]p^\varepsilon(T,x,Z)\\
&\quad+\varepsilon\left[\frac{2Vm(x,Z)}{c_o^2}\partial^2_{\frac{T}{\varepsilon}}\partial_{\frac{Z}{\varepsilon}} + 2V\partial_x m(x,Z)\partial_x\partial_{\frac{Z}{\varepsilon}}\right.\\
&\qquad\left.+\frac{1}{4}\left|\nabla_{(x,\frac{Z}{\varepsilon})}\mu_\rho\left(T,x,\frac{Z}{\varepsilon},Z\right)\right|^2\partial_{\frac{T}{\varepsilon}}\right]p^\varepsilon(T,x,Z)\\
&\quad+\text{h.o.t.} = \varepsilon^2 i\omega_o\delta'(Z)e^{-i\omega_o\frac{T}{\varepsilon}}f\left(\frac{T}{T_f},x\right)\left[1+O(\sqrt{\varepsilon})\right],
\end{aligned}
\tag{5.3}
$$

where "h.o.t." stands for higher-order terms that involve the same derivatives of p^ε as in (5.3) but with coefficients that are[1] $O(\varepsilon\sqrt{\varepsilon})$. These terms have no contribution in the limit $\varepsilon \to 0$, so we neglect them henceforth. The correction factor $1 + O(\sqrt{\varepsilon})$ in the right-hand side is also negligible as $\varepsilon \to 0$, so we neglect it as well.

Equation (5.3) holds for $T \in \mathbb{R}$ and $(x,Z) \in \mathcal{W}^\varepsilon$ with $\mathcal{W}^\varepsilon = (0,X)\times\mathbb{R}$. At the boundary $\partial\mathcal{W}^\varepsilon = \{0,X\}\times\mathbb{R}$ we obtain from (2.4), (2.6), and (5.2) that

$$
\partial_x p^\varepsilon(T,x,Z) = 0, \qquad T\in\mathbb{R},\quad (x,Z)\in\partial\mathcal{W}^\varepsilon. \tag{5.4}
$$

The initial condition (2.7) gives

$$
p^\varepsilon(T,x,Z) \equiv 0, \qquad T \ll 0,\quad (x,Z)\in\mathcal{W}^\varepsilon. \tag{5.5}
$$

5.2. Wave decomposition. We now decompose p^ε over frequencies and modes with random amplitudes that account for the long-range scattering effects.

5.2.1. Decomposition over frequencies. The decomposition over frequencies is given by the Fourier transform

$$
\widehat{p}^\varepsilon(\omega,x,Z) = \int_{-\infty}^{\infty} dT\, e^{i(\frac{\omega_o}{\varepsilon}+\omega)T} p^\varepsilon(T,x,Z) \tag{5.6}
$$

with inverse

$$
p^\varepsilon(T,x,Z) = \int_{-\infty}^{\infty}\frac{d\omega}{2\pi}\, e^{-i(\frac{\omega_o}{\varepsilon}+\omega)T}\widehat{p}^\varepsilon(\omega,x,Z). \tag{5.7}
$$

[1]Note that the velocity fluctuations $\boldsymbol{\mu_v}$ appear only in these negligible terms. Nevertheless, because the processes μ_ρ and μ_c are statistically correlated to $\boldsymbol{\mu_v}$, they play a role in the limit $\varepsilon \to 0$.

Taking the Fourier transform in (5.3), multiplying through by $-i/(\omega_o+\varepsilon\omega)$, and neglecting the higher-order terms, we obtain

$$\begin{aligned}(5.8)\quad &\Big[k^2(\omega_o+\varepsilon\omega)+\Delta_{(x,\frac{Z}{\varepsilon})}\Big]\widehat{p}^\varepsilon(\omega,x,Z)\\ &+\sqrt{\varepsilon}\int_{\mathbb{R}}\frac{d\omega'}{2\pi}\widehat{p}^\varepsilon(\omega',x,Z)\left[\widehat{Q}\left(\omega-\omega',x,\frac{Z}{\varepsilon},Z\right)-\sqrt{\varepsilon}\widehat{q}\left(\omega-\omega',x,\frac{Z}{\varepsilon},Z\right)\right]\\ &+\varepsilon\frac{2iV}{c_o}\left[k_o m(x,Z)\partial_{\frac{Z}{\varepsilon}}-\frac{1}{k_o}\partial_x m(x,Z)\partial_x\partial_{\frac{Z}{\varepsilon}}\right]\widehat{p}^\varepsilon(\omega,x,Z)\\ &=\varepsilon^2\delta'(Z)T_f\widehat{f}(\omega T_f,x),\qquad (x,Z)\in\mathcal{W}^\varepsilon.\end{aligned}$$

Here we introduced the wavenumber $k(\omega_o+\varepsilon\omega)=(\omega_o+\varepsilon\omega)/c_o$, satisfying $k(\omega_o)=k_o$, and the convolution kernel is defined by

(5.9)
$$\widehat{Q}\left(\omega,x,\frac{Z}{\varepsilon},Z\right)=\int_{-\infty}^{\infty}dT\,e^{i\omega T}\left[k_o^2\mu_c\left(T,x,\frac{Z}{\varepsilon},Z\right)+\frac{1}{2}\Delta_{(x,\frac{Z}{\varepsilon})}\mu_\rho\left(T,x,\frac{Z}{\varepsilon},Z\right)\right],$$

(5.10)
$$\widehat{q}\left(\omega,x,\frac{Z}{\varepsilon},Z\right)=\frac{1}{4}\int_{-\infty}^{\infty}dT\,e^{i\omega T}\left|\nabla_{(x,\frac{Z}{\varepsilon})}\mu_\rho\left(T,x,\frac{Z}{\varepsilon},Z\right)\right|^2.$$

The boundary condition (5.4) gives

$$(5.11)\qquad \partial_x\widehat{p}^\varepsilon(\omega,x,Z)=0,\qquad (x,Z)\in\partial\mathcal{W}^\varepsilon,$$

and $\widehat{p}^\varepsilon$ is bounded and outgoing as $|Z|\to\infty$. This radiation condition assumes that the random fluctuations are supported at finite Z. While the fluctuations may extend everywhere in the waveguide, we can restrict mathematically their support to finite Z, before taking the Fourier transform, because the causality of the wave equation and the finite speed of propagation imply that p^ε observed at $T\le T_{\max}$ is not affected by the medium at $|Z|>Z_{\max}:=\|c\|_\infty T_{\max}$.

5.2.2. Mode decomposition. The time-harmonic wave $\widehat{p}^\varepsilon$ can be decomposed further in the orthonormal $L^2([0,X])$ basis $\{\phi_j(x)\}_{j\ge 0}$ of the eigenfunctions (3.7) of the Sturm–Liouville operator $k^2(\omega_o+\varepsilon\omega)+\partial_x^2$, acting on functions of $x\in(0,X)$, with zero derivative at $x\in\{0,X\}$. The corresponding eigenvalues are

$$(5.12)\qquad \lambda_j=k^2(\omega_o+\varepsilon\omega)-\left(\frac{\pi j}{X}\right)^2,\qquad j\ge 0.$$

The decomposition is

$$(5.13)\qquad \widehat{p}^\varepsilon(\omega,x,Z)=\sum_{j=0}^{\infty}\widehat{p}_j^\varepsilon(\omega,Z)\phi_j(x),$$

where $\widehat{p}_j^\varepsilon(\omega,Z)$ are one-dimensional time-harmonic waves, the modes in the waveguide.

Substituting (5.13) in (5.8) and taking the inner product with $\phi_j(x)$, we obtain

$$\begin{aligned}(5.14)\quad &\left[k^2(\omega_o+\varepsilon\omega)-\left(\frac{\pi j}{X}\right)^2+\partial^2_{\frac{Z}{\varepsilon}}\right]\widehat{p}^\varepsilon_j(\omega,Z)\\ &+\sqrt{\varepsilon}\int_{-\infty}^{\infty}\frac{d\omega'}{2\pi}\sum_{l=0}^{\infty}\widehat{p}^\varepsilon_l(\omega',Z)\left[\widehat{\Gamma}_{j,l}\left(\omega-\omega',\frac{Z}{\varepsilon},Z\right)-\sqrt{\varepsilon}\widehat{\gamma}_{j,l}\left(\omega-\omega',\frac{Z}{\varepsilon},Z\right)\right]\\ &+\varepsilon\frac{2iV}{c_o}\sum_{l=0}^{\infty}M_{j,l}(Z)\partial_{\frac{Z}{\varepsilon}}\widehat{p}^\varepsilon_l(\omega,Z)=\varepsilon^2\delta'(Z)T_f\widehat{f}_j(\omega T_f),\qquad j\geq 0,\end{aligned}$$

where $\widehat{f}_j$ is defined in (3.13) and

$$(5.15)\qquad M_{j,l}(Z)=\int_0^X dx\,\left[k_o m(x,Z)\phi_l(x)-\frac{1}{k_o}\partial_x m(x,Z)\phi'_l(x)\right]\phi_j(x),$$

$$(5.16)\qquad \widehat{\Gamma}_{j,l}\left(\omega,\frac{Z}{\varepsilon},Z\right)=\int_0^X dx\,\widehat{Q}\left(\omega,x,\frac{Z}{\varepsilon},Z\right)\phi_j(x)\phi_l(x),$$

$$(5.17)\qquad \widehat{\gamma}_{j,l}\left(\omega,\frac{Z}{\varepsilon},Z\right)=\int_0^X dx\,\widehat{q}\left(\omega,x,\frac{Z}{\varepsilon},Z\right)\phi_j(x)\phi_l(x),\qquad j,l\geq 0.$$

5.2.3. Propagating modes. The eigenvalues (5.12) are positive for mode indexes $j\leq N(\omega_o+\varepsilon\omega)=\lfloor k(\omega_o+\varepsilon\omega)X/\pi\rfloor$, where we recall that $\lfloor\cdot\rfloor$ denotes the integer part. The corresponding modes $\widehat{p}^\varepsilon_j(\omega,Z)$ are propagating waves with wavenumbers

$$(5.18)\qquad \beta_j(\omega_o+\varepsilon\omega)=\sqrt{k^2(\omega_o+\varepsilon\omega)-\left(\frac{\pi j}{X}\right)^2},\qquad j=0,\dots,N(\omega_o+\varepsilon\omega).$$

We assume henceforth that $N(\omega_o+\varepsilon\omega)=N(\omega_o)$ and $\beta_N(\omega_o+\varepsilon\omega)>0$ for all the frequencies ω in the support of the spectrum of the source. We also simplify the notation by dropping the $\omega_o+\varepsilon\omega$ argument of N.

The propagating modes are a superposition of left- and right-going waves,

$$(5.19)\quad \widehat{p}^\varepsilon_j(\omega,Z)=\frac{1}{\sqrt{\beta_j(\omega_o+\varepsilon\omega)}}\left[a^\varepsilon_j(\omega,z)e^{i\beta_j(\omega_o+\varepsilon\omega)\frac{Z}{\varepsilon}}+b^\varepsilon_j(\omega,Z)e^{-i\beta_j(\omega_o+\varepsilon\omega)\frac{Z}{\varepsilon}}\right],$$

(5.20)

$$\partial_{\frac{Z}{\varepsilon}}\widehat{p}^\varepsilon_j(\omega,Z)=i\sqrt{\beta_j(\omega_o+\varepsilon\omega)}\left[a^\varepsilon_j(\omega,Z)e^{i\beta_j(\omega_o+\varepsilon\omega)\frac{Z}{\varepsilon}}-b^\varepsilon_j(\omega,Z)e^{-i\beta_j(\omega_o+\varepsilon\omega)\frac{Z}{\varepsilon}}\right],$$

with amplitudes $a^\varepsilon_j(\omega,Z)$ and $b^\varepsilon_j(\omega,Z)$ satisfying[2]

$$(5.21)\quad \partial_Z a^\varepsilon_j(\omega,Z)e^{i\beta_j(\omega_o+\varepsilon\omega)\frac{Z}{\varepsilon}}+\partial_Z b^\varepsilon_j(\omega,Z)e^{-i\beta_j(\omega_o+\varepsilon\omega)\frac{Z}{\varepsilon}}=0,\qquad j=0,\dots,N.$$

We are interested in the wave at $Z>0$, where the right-going modes propagate forward (away from the source), so we call $a^\varepsilon_j(\omega,Z)$ the forward-going amplitudes and $b^\varepsilon_j(\omega,Z)$ the backward-going amplitudes.

[2]The decomposition (5.19)–(5.20) is essentially the method of variation of parameters for solving a second-order inhomogeneous differential equation.

Substituting (5.19)–(5.20) in (5.14) and using (5.21), we obtain for $Z \neq 0$

$$
\begin{aligned}
(5.22)\quad & \partial_Z a_j^\varepsilon(\omega, Z) \\
&= \frac{i}{2\sqrt{\varepsilon}} \sum_{l=0}^{N} \int_{-\infty}^{\infty} \frac{d\omega'}{2\pi} \frac{\widehat{\Gamma}_{j,l}\left(\omega-\omega', \frac{Z}{\varepsilon}, Z\right)}{\sqrt{\beta_l \beta_j}} \Big[a_l^\varepsilon(\omega', Z) e^{i(\beta_l-\beta_j)\frac{Z}{\varepsilon} + i(\omega'\beta_l' - \omega\beta_j')Z} \\
&\qquad + b_l^\varepsilon(\omega', Z) e^{-i(\beta_l+\beta_j)\frac{Z}{\varepsilon} - i(\omega'\beta_l' + \omega\beta_j')Z} \Big] \\
&\quad + \frac{i}{2\sqrt{\varepsilon}} \sum_{l>N} \int_{-\infty}^{\infty} \frac{d\omega'}{2\pi} \frac{\widehat{\Gamma}_{j,l}\left(\omega-\omega', \frac{Z}{\varepsilon}, Z\right)}{\sqrt{\beta_j}} \widehat{p}_l^\varepsilon(\omega', Z) e^{-i\beta_j\frac{Z}{\varepsilon} - i\omega\beta_j' Z} \\
&\quad - \frac{i}{2} \sum_{l=0}^{N} \int_{-\infty}^{\infty} \frac{d\omega'}{2\pi} \frac{\widehat{\gamma}_{j,l}\left(\omega-\omega', \frac{Z}{\varepsilon}, Z\right)}{\sqrt{\beta_l \beta_j}} \Big[a_l^\varepsilon(\omega', Z) e^{i(\beta_l-\beta_j)\frac{Z}{\varepsilon} + i(\omega'\beta_l' - \omega\beta_j')Z} \\
&\qquad + b_l^\varepsilon(\omega', Z) e^{-i(\beta_l+\beta_j)\frac{Z}{\varepsilon} - i(\omega'\beta_l' + \omega\beta_j')Z} \Big] \\
&\quad - \frac{i}{2} \sum_{l>N} \int_{-\infty}^{\infty} \frac{d\omega'}{2\pi} \frac{\widehat{\gamma}_{j,l}\left(\omega-\omega', \frac{Z}{\varepsilon}, Z\right)}{\sqrt{\beta_j}} \widehat{p}_l^\varepsilon(\omega', Z) e^{-i\beta_j\frac{Z}{\varepsilon} - i\omega\beta_j' Z} \\
&\quad - \frac{iV}{c_o} \sum_{l=0}^{N} \frac{\sqrt{\beta_l}}{\sqrt{\beta_j}} M_{j,l}(Z) \Big[a_l^\varepsilon(\omega, Z) e^{i(\beta_l-\beta_j)\frac{Z}{\varepsilon} + i\omega(\beta_l' - \beta_j')Z} \\
&\qquad - b_l^\varepsilon(\omega, Z) e^{-i(\beta_l+\beta_j)\frac{Z}{\varepsilon} - i\omega(\beta_l' + \beta_j')Z} \Big] \\
&\quad - \frac{V}{c_o} \sum_{l>N} \frac{M_{j,l}(Z)}{\sqrt{\beta_j}} \partial_{\frac{Z}{\varepsilon}} \widehat{p}_l^\varepsilon(\omega, Z) e^{-i\beta_j\frac{Z}{\varepsilon} - i\omega\beta_j' Z} + \text{h.o.t.}
\end{aligned}
$$

and

$$
(5.23)\qquad \partial_Z b_j^\varepsilon(\omega, Z) = -\partial_Z a_j^\varepsilon(\omega, Z) e^{2i\beta_j\frac{Z}{\varepsilon} + 2i\omega\beta_j' Z} + \text{h.o.t.}
$$

Here we used the notation (3.8), and "h.o.t." denotes, as before, higher-order terms that are negligible as $\varepsilon \to 0$.

Equations (5.22)–(5.23) show that the propagating mode amplitudes are coupled with each other and the evanescent modes via the matrices (5.16)–(5.15) defined by the random fluctuations. They are complemented with the boundary conditions[3]

$$
(5.24)\qquad a_j^\varepsilon(\omega, Z = 0^+) = a_{j,o}(\omega) = \frac{\sqrt{\beta_j} T_f}{2} \widehat{f}_j(\omega T_f),
$$

$$
(5.25)\qquad b_j^\varepsilon(\omega, Z = Z_{\max}) = 0, \qquad j = 0, \dots, N.
$$

Note that the right-hand side in (5.24) equals the amplitude of the jth propagating mode in the ideal waveguide; this incoming condition follows since the random fluctuations have an effect on the mode only for positive range. Condition (5.25) ensures that the wave is outgoing at $Z > Z_{\max}$, where we recall that $Z_{\max}$ is the range at which we truncate mathematically the support of the random fluctuations.

[3] For the wave at $Z < 0$ we have the analogue of (5.24)–(5.25), where $b_j^\varepsilon(\omega, Z = 0^-)$ is determined by the source and $a_j^\varepsilon(\omega, Z = -Z_{\max}) = 0$.

5.2.4. Evanescent modes. The modes indexed by $j > N$ are evanescent waves, corresponding to the negative eigenvalues (5.12), which define the decay rates

$$\beta_j(\omega_o + \varepsilon\omega) = \sqrt{\left(\frac{\pi j}{X}\right)^2 - k^2(\omega_o + \varepsilon\omega)}, \qquad j > N. \tag{5.26}$$

These modes can be expressed in terms of the propagating ones, as we now explain.

With $\widehat{G}_j^\varepsilon(\omega, Z) = \exp[-\beta_j(\omega_o + \varepsilon\omega)\frac{|Z|}{\varepsilon}]/[2\beta_j(\omega_o + \varepsilon\omega)]$, the Green's function in equation

$$\left[\partial^2_{\frac{Z}{\varepsilon}} - \beta_j^2(\omega_o + \varepsilon\omega)\right]\widehat{G}_j^\varepsilon(\omega, Z) = -\delta\left(\frac{Z}{\varepsilon}\right), \qquad \lim_{|Z|/\varepsilon\to\infty} \widehat{G}_j^\varepsilon(\omega, Z) = 0,$$

we transform (5.14) for $j > N$ into the following system of integral equations:

$$\begin{aligned}\left[\left(I - \sqrt{\varepsilon}\mathscr{L}^{\mathrm{ev}}\right)\widehat{\boldsymbol{p}}^\varepsilon\right]_j(\omega, Z) = \sqrt{\varepsilon}\int_{-\infty}^{\infty} d\zeta\, \frac{e^{-\beta_j|\zeta|}}{2\beta_j} \\ \times \sum_{l=0}^{N}\int_{-\infty}^{\infty}\frac{d\omega'}{2\pi}\,\widehat{p}_l^\varepsilon(\omega', Z + \varepsilon\zeta)\widehat{\Gamma}_{j,l}\left(\omega - \omega', \frac{Z}{\varepsilon} + \zeta, Z\right) + \text{h.o.t.}\end{aligned} \tag{5.27}$$

Here we used the notation (3.8) and introduced the vector $\widehat{\boldsymbol{p}}^\varepsilon = (\widehat{p}_l^\varepsilon(\omega, Z))_{\omega, Z\in\mathbb{R}, l>N}$ with infinitely many components given by the evanescent modes. The symbol $[\cdot]_j$ means taking the jth component, I is the identity, and $\mathscr{L}^{\mathrm{ev}}$ is the linear integral operator acting on square summable sequences of continuous functions of Z given by

$$\left[\mathscr{L}^{\mathrm{ev}}\widehat{\boldsymbol{p}}^\varepsilon\right]_j(\omega, Z) = \int_{-\infty}^{\infty} d\zeta\, \frac{e^{-\beta_j|\zeta|}}{2\beta_j}\sum_{l>N}\int_{-\infty}^{\infty}\frac{d\omega'}{2\pi}\,\widehat{p}_l^\varepsilon(\omega', Z + \varepsilon\zeta)\widehat{\Gamma}_{j,l}\left(\omega - \omega', \frac{Z}{\varepsilon} + \zeta, Z\right).$$

This operator is of the same form as in [10, section 20.2.3] and it is bounded. Therefore, we can express the evanescent modes in terms of the propagating ones by inverting (5.27) using Neumann series:

$$\begin{aligned}\widehat{p}_j^\varepsilon(\omega, Z) = \sqrt{\varepsilon}\int_{-\infty}^{\infty} d\zeta \frac{e^{-\beta_j|\zeta|}}{2\beta_j} \\ \times \sum_{l=0}^{N}\int_{-\infty}^{\infty}\frac{d\omega'}{2\pi}\widehat{p}_l^\varepsilon(\omega', Z + \varepsilon\zeta)\widehat{\Gamma}_{j,l}\left(\omega - \omega', \frac{Z}{\varepsilon} + \zeta, Z\right) + \text{h.o.t.}\end{aligned}$$

Recalling the decomposition (5.19) of the propagating modes and observing that due to the decaying exponential in the ζ integral only $|\zeta| = O(1)$ contributes, we can write this expression as

$$\begin{aligned}\widehat{p}_j^\varepsilon(\omega, Z) = \sqrt{\varepsilon}\int_{\mathbb{R}} d\zeta \frac{e^{-\beta_j|\zeta|}}{2\beta_j}\sum_{l=0}^{N}\frac{1}{\sqrt{\beta_l}}\int_{-\infty}^{\infty}\frac{d\omega'}{2\pi}\widehat{\Gamma}_{j,l}\left(\omega - \omega', \frac{Z}{\varepsilon} + \zeta, Z\right) \\ \times\left[a_l^\varepsilon(\omega', Z)e^{i\beta_l\frac{Z}{\varepsilon} + i\beta_l\zeta + i\omega'\beta_l' Z} + b_l^\varepsilon(\omega', Z)e^{-i\beta_l\frac{Z}{\varepsilon} - i\beta_l\zeta - i\omega'\beta_l' Z}\right] + \text{h.o.t.}\end{aligned} \tag{5.28}$$

for $j > N$ because by (5.22)–(5.23) we have

$$a_l^\varepsilon(\omega', Z + \varepsilon\zeta) = a_l^\varepsilon(\omega', Z) + O(\sqrt{\varepsilon}), \qquad l = 0, \ldots, N,$$

and similar for $b_l^\varepsilon(\omega', Z + \varepsilon\zeta)$.

5.3. Asymptotic analysis of the mode amplitudes. The substitution of (5.28) in (5.22)–(5.23) gives a closed system of $2(N+1)$ equations for the propagating mode amplitudes. In the limit $\varepsilon \to 0$, this system can be simplified further under the assumption that the correlation functions (3.1)–(3.4) are smooth enough in ζ. This leads to the forward scattering approximation described in section 5.3.1. The $\varepsilon \to 0$ limit of the mode amplitudes under this approximation is obtained in section 5.3.2.

5.3.1. Forward scattering approximation. In the limit $\varepsilon \to 0$, the backward-going mode amplitudes $\{b_j^\varepsilon(\omega, Z)\}_{0\le j\le N}$ are coupled to $\{a_j^\varepsilon(\omega, Z)\}_{0\le j\le N}$ via terms that are proportional to the power spectral densities [10, section 20.2.6]

$$\widehat{\mathcal{R}}_{\alpha\alpha'}(\omega, x, x', \kappa, Z) = \int_{-\infty}^{\infty} d\tau \int_{-\infty}^{\infty} d\zeta \; e^{i\omega\tau - i\kappa\zeta} \mathcal{R}_{\alpha\alpha'}(\tau, x, x', \zeta, Z) \tag{5.29}$$

evaluated at $\kappa = \beta_j + \beta_{j'}$ for $j, j' = 0, \ldots, N$ and $\alpha, \alpha' \in \{\rho, c\}$. When the support in κ of $\widehat{\mathcal{R}}_{\alpha\alpha'}$ is smaller than $2\beta_N$, this coupling is negligible. Since $\{b_j^\varepsilon(\omega, Z)\}_{0\le j\le N}$ satisfy the homogeneous boundary condition (5.25) at $Z = Z_{\max}$, we can set

$$b_j^\varepsilon(\omega, Z) \approx 0, \qquad Z > 0, \quad j = 0, \ldots, N. \tag{5.30}$$

The forward-going amplitudes are coupled in the limit $\varepsilon \to 0$, as shown in the next section, and they satisfy the initial value problem

$$\partial_Z \boldsymbol{a}^\varepsilon(\omega, Z) = \int_{-\infty}^{\infty} \frac{d\omega'}{2\pi} \left[\frac{1}{\sqrt{\varepsilon}} \mathbf{H}\left(\omega, \omega', \frac{Z}{\varepsilon}, \frac{Z}{\varepsilon}, Z\right) + \mathbf{h}\left(\omega, \omega', \frac{Z}{\varepsilon}, \frac{Z}{\varepsilon}, Z\right)\right] \boldsymbol{a}^\varepsilon(\omega', Z) \tag{5.31}$$

at $Z > 0$ with initial condition $\boldsymbol{a}^\varepsilon(\omega, Z = 0^+) = \boldsymbol{a}_o(\omega)$. Here $\boldsymbol{a}^\varepsilon(\omega, Z)$ is the $N+1$ vector field with components $a_j^\varepsilon(\omega, z)$, and the components of $\boldsymbol{a}_o(\omega)$ are the initial mode amplitudes $a_{j,o}(\omega)$ defined in (5.24). Moreover, the $(N+1)\times(N+1)$ coupling matrices $\mathbf{H}$ and $\mathbf{h}$ have the entries

$$H_{j,l}(\omega, \omega', \zeta, \xi, Z) = \frac{i}{2\sqrt{\beta_j \beta_l}} \widehat{\Gamma}_{j,l}(\omega - \omega', \zeta, Z) e^{i(\beta_l - \beta_j)\xi + i(\omega'\beta_l' - \omega\beta_j')Z}, \tag{5.32}$$

and

$$\begin{aligned} h_{j,l}(\omega, \omega', \zeta, \xi, Z) = e^{i(\beta_l - \beta_j)\xi + i(\omega'\beta_l' - \omega\beta_j')Z} \Bigg[&- \frac{i}{2\sqrt{\beta_j\beta_l}} \widehat{\gamma}_{j,l}(\omega - \omega', \zeta, Z) \\ &- \frac{i2\pi V}{c_o} \delta(\omega - \omega') \frac{\sqrt{\beta_l}}{\sqrt{\beta_j}} M_{j,l}(Z) \\ &+ \frac{i}{4} \sum_{r>N} \frac{1}{\beta_r \sqrt{\beta_j\beta_l}} \int_{-\infty}^{\infty} \frac{d\omega''}{2\pi} \int_{-\infty}^{\infty} ds \, e^{-\beta_r|s| + i\beta_l s} \\ &\times \widehat{\Gamma}_{j,r}(\omega - \omega' - \omega'', \zeta, z) \widehat{\Gamma}_{r,l}(\omega'', \zeta + s, Z) \Bigg] \end{aligned} \tag{5.33}$$

for $j, l = 0, \ldots, N$. The last term in (5.33) is due to the evanescent modes.

Note that definitions (5.9)–(5.10), (5.16)–(5.17), and (5.32)–(5.33) imply that

$$\mathbf{H}^\dagger(\omega', \omega, \zeta, \xi, Z) = -\mathbf{H}(\omega, \omega', \zeta, \xi, Z), \qquad \mathbf{h}^\dagger(\omega', \omega, \zeta, \xi, Z) \neq -\mathbf{h}(\omega, \omega', \zeta, \xi, Z),$$

where † stands for conjugate transpose. Thus, energy is not conserved at finite ε,

$$\partial_Z \int_{-\infty}^{\infty} \frac{d\omega}{2\pi} \left|\boldsymbol{a}^\varepsilon(\omega, Z)\right|^2 = \iint_{-\infty}^{\infty} \frac{d\omega}{2\pi}\frac{d\omega'}{2\pi} \boldsymbol{a}^\varepsilon(\omega, Z)^\dagger \Big[\mathbf{h}^\dagger\Big(\omega', \omega, \frac{Z}{\varepsilon}, \frac{Z}{\varepsilon}, Z\Big) + \mathbf{h}\Big(\omega, \omega', \frac{Z}{\varepsilon}, \frac{Z}{\varepsilon}, Z\Big)\Big] \boldsymbol{a}^\varepsilon(\omega', Z) \neq 0,$$

due to the flow and the interaction with the evanescent waves. However, only the diagonal part of the second-order coupling matrix $\mathbf{h}$ contributes in the limit $\varepsilon \to 0$ (see the next section and Appendix B), and it satisfies

$$\mathrm{diag}\Big[\mathbf{h}^\dagger(\omega', \omega, \zeta, \xi, Z) + \mathbf{h}(\omega, \omega', \zeta, \xi, Z)\Big] = 0.$$

This gives the conservation of energy of the propagating modes in the limit $\varepsilon \to 0$.

We also note that the effective coupling coefficients of the forward-going mode amplitudes (see Appendix B) depend on the parameters $\widehat{\mathcal{R}}_{\alpha\alpha'}(\omega, x, x', \kappa, Z)$ defined by (5.29) and evaluated at $\kappa = \beta_j - \beta_{j'}$ for $j, j' = 0, \ldots, N$ and $\alpha, \alpha' \in \{\rho, c\}$. Some of these coupling parameters (in particular, those for which $|j - j'| = 1$) can be significant, and that is why there is coupling between forward-going modes in the forward scattering approximation.

5.3.2. Markovian limit. Definitions (5.9), (5.16), and (5.32) give that

$$\mathbb{E}\Big[\mathbf{H}(\omega, \omega', \zeta, \xi, Z)\Big] = 0 \qquad \forall \omega, \omega' \in \mathbb{R}, \ \ \forall \zeta, \xi, Z \in \mathbb{R}^+, \tag{5.34}$$

and $\varepsilon \to 0$ in (5.31) corresponds to a diffusion limit. Specifically, we have that

$$\boldsymbol{A}^\varepsilon(Z) = \Big(\boldsymbol{a}^\varepsilon(\omega, Z)\Big)_{\omega \in \mathbb{R}} \overset{\varepsilon \to 0}{\longrightarrow} \boldsymbol{A}(Z) = \Big(\boldsymbol{a}(\omega, Z)\Big)_{\omega \in \mathbb{R}}, \tag{5.35}$$

where the convergence is in distribution in $\mathcal{C}^0([0, Z_{\max}], \mathcal{D}')$. The limit $\boldsymbol{A}(Z)$ is an inhomogeneous Markov process with infinitesimal generator $\mathcal{L}_Z$ defined in Appendix B, following the method described in [6, Appendix A]. With this generator we can compute all the statistical moments of the limit mode amplitudes. Here we explain how to obtain the first two moments, which are stated in section 3 and are used to solve the inverse problems in section 4.

To calculate the mean mode amplitudes, let $\widehat{\varphi}_j(\omega)$ be smooth functions of ω for $j = 0, \ldots, N$, and define the test functions $f_{j,\varphi}$:

$$f_{j,\varphi}(\boldsymbol{A}, \overline{\boldsymbol{A}}) = \int_{-\infty}^{\infty} d\omega\, \widehat{\varphi}_j(\omega) a_j(\omega), \qquad \boldsymbol{A} = \big(a_j(\omega)\big)_{j=0,\ldots,N, \omega \in \mathbb{R}}. \tag{5.36}$$

Using the expression (B.2) of $\mathcal{L}_Z$ we find

$$\mathcal{L}_Z f_{j,\varphi}(\boldsymbol{A}, \overline{\boldsymbol{A}}) = \int_{-\infty}^{\infty} d\omega\, \widehat{\varphi}_j(\omega) a_j(\omega) \Big[\Theta_j(Z) + i\Psi_j(Z) - \frac{iV}{c_o} M_{jj}(Z)\Big]$$

with M_{jj}, Θ_j, and Ψ_j defined in (3.15)–(3.17). The expectation (3.12) of the limit mode amplitudes follows from this expression and Kolmogorov's equation.

The expression of the Wigner transform (3.22) involves the second moments $\mathbb{E}[a_j(\omega, Z)\overline{a}_j(\omega', Z)]$ of the amplitudes. These are obtained by applying the generator (B.2) to test functions of the form

$$f_{j,l,\varphi}(\boldsymbol{A}, \overline{\boldsymbol{A}}) = \iint_{-\infty}^{\infty} d\omega\, d\omega'\, \widehat{\varphi}(\omega, \omega') a_j(\omega)\overline{a}_l(\omega').$$

6. Summary. We introduced an analysis of sound propagation in a waveguide filled with a random medium that depends on time due to a weakly turbulent flow at speed $\boldsymbol{v}(t, \boldsymbol{x})$. The medium is modeled by random fluctuations of the mass density and sound speed, which are statistically correlated to the fluctuations of $\boldsymbol{v}(t, \boldsymbol{x})$. The analysis is based on the wave equation satisfied by the pressure $p(t, \boldsymbol{x})$, obtained from the linearization of the fluid dynamics equations about the flow. It involves the decomposition of $p(t, \boldsymbol{x})$ in propagating and evanescent modes, which are time-harmonic waves with random amplitudes that model scattering in the random medium. These amplitudes are described in a forward scattering regime, using the diffusion-approximation theory. We showed how to use their first two statistical moments to estimate the flow from measurements of $p(t, \boldsymbol{x})$ at an array of receivers.

Appendix A. Compatibility of the weakly turbulent flow model. We explain in this appendix that the model (2.9)–(2.10) of the weakly turbulent flow is compatible with the basic equations (2.2)–(2.3).

By substitution of the ansätze (2.9)–(2.10) in (2.2)–(2.3) and by collecting the leading-order terms in ε we get the equations

$$V\nabla_{\boldsymbol{x}} \cdot \boldsymbol{\mu}_{\boldsymbol{v}}(T, \boldsymbol{x}, Z) + \big(\partial_T + Vm(x, Z)\partial_z\big)\mu_\rho(T, \boldsymbol{x}, Z) = 0,$$
$$\big(\partial_T + Vm(x, Z)\partial_z\big)\mu_c(T, \boldsymbol{x}, Z) + \frac{\rho_o}{c_o^2}\left(\frac{\partial^2 P}{\partial \rho^2}\right)_0 \big(\partial_T + Vm(x, Z)\partial_z\big)\mu_\rho(T, \boldsymbol{x}, Z) = 0,$$

for $\boldsymbol{x} = (x, z)$, where $\nabla_{\boldsymbol{x}} = (\partial_x, \partial_z)$. This shows that the processes μ_ρ, μ_c are of the form

$$\mu_\rho(T, \boldsymbol{x}, Z) = \nu_\rho(T, x, z - Vm(x, Z)T, Z), \tag{A.1}$$
$$\mu_c(T, \boldsymbol{x}, Z) = \nu_c(T, x, z - Vm(x, Z)T, Z). \tag{A.2}$$

Moreover, $\boldsymbol{\mu}_{\boldsymbol{v}}$ can be written as

$$\boldsymbol{\mu}_{\boldsymbol{v}}(T, \boldsymbol{x}, Z) = \nabla_{\boldsymbol{x}}\nu_{\boldsymbol{v}}(T, x, z - Vm(x, Z)T, Z) + \nabla_{\boldsymbol{x}}^{\perp}\widetilde{\nu}_{\boldsymbol{v}}(T, x, z - Vm(x, Z)T, Z),$$

where $\nabla_{\boldsymbol{x}}^{\perp} = (-\partial_z, \partial_x)^T$. The real-valued $\nu_\rho, \nu_c, \nu_{\boldsymbol{v}}$ in these expressions satisfy

$$V\Delta_{(x,z)}\nu_{\boldsymbol{v}}(T, x, z, Z) + \partial_T\nu_\rho(T, x, z, Z) = 0, \tag{A.3}$$
$$\partial_T\nu_c(T, x, z, Z) + \frac{\rho_o}{c_o^2}\left(\frac{\partial^2 P}{\partial \rho^2}\right)_0 \partial_T\nu_\rho(T, x, z, Z) = 0, \tag{A.4}$$

and the boundary conditions

$$\partial_x\nu_\rho(T, \boldsymbol{x}, Z) = \partial_x\nu_c(T, \boldsymbol{x}, Z) = \partial_x\nu_{\boldsymbol{v}}(T, \boldsymbol{x}, Z) = 0, \qquad \boldsymbol{x} \in \partial\mathcal{W}. \tag{A.5}$$

We now show that there exist particular solutions to these equations.

Let us fix Z and introduce the Fourier transform of ν_ρ,

$$\widehat{\nu}_\rho(\omega, x, \kappa, Z) = \int_{-\infty}^{\infty} dT \int_{-\infty}^{\infty} dz\, \nu_\rho(T, x, z, Z) e^{i\omega T - i\kappa z} = \sum_{j=0}^{\infty} \widehat{\nu}_{\rho,j}(\omega, \kappa, Z)\phi_j(x),$$

where we used the basis $\{\phi_j(x)\}_{j\geq 0}$ to ensure that (A.5) holds and introduced the independent processes $\widehat{\nu}_{\rho,j}$ with mean zero and covariance functions

$$\mathbb{E}\big[\overline{\widehat{\nu}_{\rho,j}}(\omega, \kappa, Z)\widehat{\nu}_{\rho,j'}(\omega', \kappa', Z)\big] = \delta_{jj'}\delta(\omega - \omega')\delta(\kappa - \kappa')\widehat{F}_{\rho,j}(\omega, \kappa, Z).$$

The power spectral densities $\widehat{F}_{\rho,j}$ are assumed to decay fast at infinity as functions of ω and κ. Moreover, $\widehat{F}_{\rho,j}$ are bounded by $C(\omega)\kappa^4$ for κ close to zero with $C(\omega)$ decaying fast at infinity.

Consider $\widetilde{\nu}_{\boldsymbol{v}} = 0$. Then we can find ν_c and $\nu_{\boldsymbol{v}}$ stationary in T and z that are compatible with (A.3)–(A.4):

$$\widehat{\nu}_c(\omega, x, \kappa, Z) = \sum_{j=0}^{\infty} \widehat{\nu}_{c,j}(\omega, \kappa, Z)\phi_j(x), \quad \widehat{\nu}_{c,j}(\omega, \kappa, Z) = -\frac{\rho_o}{c_o^2}\left(\frac{\partial^2 P}{\partial \rho^2}\right)_0 \widehat{\nu}_{\rho,j}(\omega, \kappa, Z),$$
$$\widehat{\nu}_{\boldsymbol{v}}(\omega, x, \kappa, Z) = \sum_{j=0}^{\infty} \widehat{\nu}_{\boldsymbol{v},j}(\omega, \kappa, Z)\phi_j(x), \quad \widehat{\nu}_{\boldsymbol{v},j}(\omega, \kappa, Z) = -\frac{i\omega}{V(j^2+\kappa^2)}\widehat{\nu}_{\rho,j}(\omega, \kappa, Z).$$

These are not the only possible solutions. This is why we consider the general form (2.9)–(2.10) of the fluctuations with the random processes μ_ρ, $\boldsymbol{\mu}_{\boldsymbol{v}}$, and μ_c that are correlated (with an arbitrary correlation) and stationary in T and z.

Appendix B. Generator of the limit Markov process. The limit $\varepsilon \to 0$ is obtained as described in [6, Appendix A]. Here we give the expression of the generator.

For any $\boldsymbol{A} = (a_j(\omega))_{j=0,\dots,N,\omega\in\mathbb{R}}$, any smooth function $\widehat{\varphi} : \mathbb{R}^{m+n} \to \mathbb{R}$, and any vector of integers $\boldsymbol{d} = (d_l)_{l=1}^{n+m}$ in $\{0, \dots, N\}^{n+m}$, define the test function

$$f_{\boldsymbol{d},\varphi}(\boldsymbol{A}, \overline{\boldsymbol{A}}) = \int_{-\infty}^{\infty} \cdots \int_{-\infty}^{\infty} \widehat{\varphi}(\omega_1, \dots, \omega_{n+m}) \prod_{l=1}^{n} a_{d_l}(\omega_l) \prod_{l=n+1}^{n+m} \overline{a}_{d_l}(\omega_l) \prod_{l=1}^{n+m} d\omega_l.$$

Its variational derivatives are, for $j = 0, \dots, N$,

$$\frac{\delta f_{\boldsymbol{d},\varphi}}{\delta a_j(\omega)} = \sum_{r\in J_j} \int_{-\infty}^{\infty} \cdots \int_{-\infty}^{\infty} \widehat{\varphi}(\omega_1, \dots, \omega_{n+m})|_{\omega_r=\omega} \prod_{l=1, l\neq r}^{n} a_{d_l}(\omega_l) \prod_{l=n+1}^{n+m} \overline{a}_{d_l}(\omega_l) \prod_{l=1, l\neq r}^{n+m} d\omega_l,$$
$$\frac{\delta f_{\boldsymbol{d},\varphi}}{\delta \overline{a}_j(\omega)} = \sum_{r\in J'_j} \int_{-\infty}^{\infty} \cdots \int_{-\infty}^{\infty} \widehat{\varphi}(\omega_1, \dots, \omega_{n+m})|_{\omega_r=\omega} \prod_{l=1}^{n} a_{d_l}(\omega_l) \prod_{l=n+1, l\neq r}^{n+m} \overline{a}_{d_l}(\omega_l) \prod_{l=1, l\neq r}^{n+m} d\omega_l,$$

where $J_j = \{l = 1, \dots, n, d_l = j\}$ and $J'_j = \{l = n+1, \dots, n+m, d_l = j\}$.

The generator is the operator $\mathcal{L}_Z$ acting on these functions, defined by

$$\begin{aligned}
\mathcal{L}_Z f_{\boldsymbol{d},\varphi}(\boldsymbol{A},\overline{\boldsymbol{A}}) &= \int_0^\infty d\zeta \lim_{z_o\to\infty}\frac{1}{z_o}\int_0^{z_o} ds \iiiint_{-\infty}^{\infty} d\omega_1' d\omega_2' d\omega_1 d\omega_2 \sum_{j,l,r,q=0}^{N}\frac{1}{4\pi^2}\\
&\times\Big\{\mathbb{E}\big[\overline{H_{l,j}}(\omega_1',\omega_1,0,s,Z)\overline{H_{q,r}}(\omega_2',\omega_2,\zeta,\zeta+s,Z)\big]\frac{\delta^2 f_{\boldsymbol{d},\varphi}}{\delta\overline{a}_l(\omega_1')\delta\overline{a}_q(\omega_2')}\overline{a}_j(\omega_1)\overline{a}_r(\omega_2)\\
&\quad+\mathbb{E}\big[\overline{H_{l,j}}(\omega_1',\omega_1,0,s,Z)H_{q,r}(\omega_2',\omega_2,\zeta,\zeta+s,Z)\big]\frac{\delta^2 f_{\boldsymbol{d},\varphi}}{\delta\overline{a}_l(\omega_1')\delta a_q(\omega_2')}\overline{a}_j(\omega_1)a_r(\omega_2)\\
&\quad+\mathbb{E}\big[H_{l,j}(\omega_1',\omega_1,0,s,Z)\overline{H_{q,r}}(\omega_2',\omega_2,\zeta,\zeta+s,Z)\big]\frac{\delta^2 f_{\boldsymbol{d},\varphi}}{\delta a_l(\omega_1')\delta\overline{a}_q(\omega_2')}a_j(\omega_1)\overline{a}_r(\omega_2)\\
&\quad+\mathbb{E}\big[H_{l,j}(\omega_1',\omega_1,0,s,Z)H_{q,r}(\omega_2',\omega_2,\zeta,\zeta+s,Z)\big]\frac{\delta^2 f_{\boldsymbol{d},\varphi}}{\delta a_l(\omega_1')\delta a_q(\omega_2')}a_j(\omega_1)a_r(\omega_2)\Big\}\\
&+\int_0^\infty d\zeta \lim_{z_o\to\infty}\frac{1}{z_o}\int_0^{z_o} ds\iiint_{-\infty}^{\infty} d\omega_1' d\omega_1 d\omega' \sum_{j,q,l=0}^{N}\frac{1}{4\pi^2}\\
&\times\Big\{\mathbb{E}\big[\overline{H}_{l,j}(\omega_1',\omega_1,0,s,Z)\overline{H}_{q,l}(\omega',\omega_1',\zeta,\zeta+s,Z)\big]\frac{\delta f_{\boldsymbol{d},\varphi}}{\delta\overline{a}_q(\omega')}\overline{a}_j(\omega_1)\\
&\quad+\mathbb{E}\big[H_{l,j}(\omega_1',\omega_1,0,s,Z)H_{q,l}(\omega',\omega_1',\zeta,\zeta+s,Z)\big]\frac{\delta f_{\boldsymbol{d},\varphi}}{\delta a_q(\omega')}a_j(\omega_1)\Big\}\\
&+\lim_{z_o\to\infty}\frac{1}{z_o}\int_0^{z_o} ds\iint_{-\infty}^{\infty} d\omega_1 d\omega_1'\sum_{j,q=0}^{N}\frac{1}{2\pi}\Big\{\mathbb{E}\big[\overline{h}_{qj}(\omega_1',\omega_1,0,s,Z)\big]\frac{\delta f_{\boldsymbol{d},\varphi}}{\delta\overline{a}_q(\omega_1')}\overline{a}_j(\omega_1)\\
&\quad+\mathbb{E}\big[h_{qj}(\omega_1',\omega_1,0,s,Z)\big]\frac{\delta f_{\boldsymbol{d},\varphi}}{\delta a_q(\omega_1')}a_j(\omega_1)\Big\}.
\end{aligned}\tag{B.1}$$

Using definitions (5.32)–(5.33) in (B.1) and for $\boldsymbol{A}$ as in (5.36), we obtain after long but elementary calculations that

$$\begin{aligned}
\mathcal{L}_Z f_{\boldsymbol{d},\varphi}(\boldsymbol{A},\overline{\boldsymbol{A}}) = \iiiint_{-\infty}^{\infty} d\omega_1' d\omega_2' d\omega_1 d\omega_2 &\sum_{j,l,r,q=0}^{N}\\
&\times\Big\{\overline{\overline{\eta}}_{j,l,r,q}(\omega_1',\omega_2',\omega_1,\omega_2,Z)\frac{\delta^2 f_{\boldsymbol{d},\varphi}}{\delta\overline{a}_l(\omega_1')\delta\overline{a}_q(\omega_2')}\overline{a}_j(\omega_1)\overline{a}_r(\omega_2)\\
&\quad+\eta_{j,l,r,q}(\omega_1',\omega_2',\omega_1,\omega_2,Z)\frac{\delta^2 f_{\boldsymbol{d},\varphi}}{\delta\overline{a}_l(\omega_1')\delta a_q(\omega_2')}\overline{a}_j(\omega_1)a_r(\omega_2)\\
&\quad+\overline{\eta}_{j,l,r,q}(\omega_1',\omega_2',\omega_1,\omega_2,Z)\frac{\delta^2 f_{\boldsymbol{d},\varphi}}{\delta a_l(\omega_1')\delta\overline{a}_q(\omega_2')}a_j(\omega_1)\overline{a}_r(\omega_2)\\
&\quad+\widetilde{\eta}_{j,l,r,q}(\omega_1',\omega_2',\omega_1,\omega_2,Z)\frac{\delta^2 f_{\boldsymbol{d},\varphi}}{\delta a_l(\omega_1')\delta a_q(\omega_2')}a_j(\omega_1)a_r(\omega_2)\Big\}\\
&+\iint_{-\infty}^{\infty} d\omega_1' d\omega_1\sum_{j,q=0}^{N}\Big\{\overline{\sigma}_{jq}(\omega_1',\omega_1,Z)\frac{\delta f_{\boldsymbol{d},\varphi}}{\delta\overline{a}_q(\omega_1')}\overline{a}_j(\omega_1)\\
&\qquad+\sigma_{jq}(\omega_1',\omega_1,Z)\frac{\delta f_{\boldsymbol{d},\varphi}}{\delta a_q(\omega_1')}a_j(\omega_1)\Big\}
\end{aligned}\tag{B.2}$$

with tensor-valued integral kernels defined in terms of

$$\begin{aligned}\mathcal{C}_{j,l,r,q}(\tau,\zeta,Z)&\\ =\iint_0^X dxdx'\,\phi_j\phi_l(x)\phi_r\phi_q(x')&\\ \Big[k_o^4\mathcal{R}_{cc}(\tau,x,x',\zeta,Z)+\frac{k_o^2}{2}(\partial_\zeta^2+\partial_{x'}^2)\mathcal{R}_{c\rho}(\tau,x,x',\zeta,Z)&\\ +\frac{k_o^2}{2}(\partial_\zeta^2+\partial_x^2)\mathcal{R}_{\rho c}(\tau,x,x',\zeta,Z)&\\ +\frac{1}{4}(\partial_\zeta^2+\partial_x^2)(\partial_\zeta^2+\partial_{x'}^2)\mathcal{R}_{\rho\rho}(\tau,x,x',\zeta,Z)\Big].&\end{aligned} \tag{B.3}$$

These kernels are

$$\begin{aligned}\eta_{j,l,r,q}(\omega_1',\omega_2',\omega_1,\omega_2,z)=&\frac{1}{8\pi\sqrt{\beta_j\beta_l\beta_r\beta_q}}\left[\delta_{jl}\delta_{rq}+(1-\delta_{jl})\delta_{jr}\delta_{lq}\right]\\ &\times\delta(\omega_1-\omega_1'+\omega_2'-\omega_2)e^{i(\omega_1'\beta_l'-\omega_1\beta_j'+\omega_2\beta_r'-\omega_2'\beta_q')Z}\\ &\times\int_0^\infty d\zeta\int_{-\infty}^\infty d\tau\,\mathcal{C}_{j,l,r,q}(\tau,\zeta,Z)e^{i(\omega_2'-\omega_2)\tau+i(\beta_r-\beta_q)\zeta},\end{aligned} \tag{B.4}$$

$$\begin{aligned}\widetilde{\eta}_{j,l,r,q}(\omega_1',\omega_2',\omega_1,\omega_2,Z)=&-\frac{1}{8\pi\sqrt{\beta_j\beta_l\beta_r\beta_q}}\left[\delta_{jl}\delta_{rq}+(1-\delta_{jl})\delta_{jr}\delta_{lq}\right]\\ &\times\delta(\omega_1'-\omega_1+\omega_2'-\omega_2)e^{i(-\omega_1'\beta_l'+\omega_1\beta_j'+\omega_2\beta_r'-\omega_2'\beta_q')Z}\\ &\times\int_0^\infty d\zeta\int_{-\infty}^\infty d\tau\,\mathcal{C}_{j,l,r,q}(\tau,\zeta,Z)e^{i(\omega_2'-\omega_2)\tau+i(\beta_r-\beta_q)\zeta},\end{aligned} \tag{B.5}$$

$$\sigma_{jq}(\omega_1,\omega_1',Z)=\delta_{jq}\delta(\omega_1-\omega_1')\left[\Theta_j(Z)+i\Psi_j(Z)-i\frac{VM_{jj}(Z)}{c_o}\right], \tag{B.6}$$

with M_{jj},Θ_j and Ψ_j defined in (3.15)–(3.17).

REFERENCES

[1] A. Aisopou, I. Stoianov, and N. J. Graham, *In-pipe water quality monitoring in water supply systems under steady and unsteady state flow conditions: A quantitative assessment*, Water Res., 46 (2012), pp. 235–246.

[2] R. Alonso and L. Borcea, *Electromagnetic wave propagation in random waveguides*, SIAM Multiscale Model. Simul., 13 (2015), pp. 847–889.

[3] R. Alonso, L. Borcea, and J. Garnier, *Wave propagation in waveguides with random boundaries*, Commun. Math. Sci., 11 (2012), pp. 233–267.

[4] L. Borcea and J. Garnier, *Paraxial coupling of propagating modes in three-dimensional waveguides with random boundaries*, SIAM Multiscale Model. Simul., 12 (2014), pp. 832–878.

[5] L. Borcea and J. Garnier, *Pulse reflection in a random waveguide with a turning point*, SIAM Multiscale Model. Simul., 15 (2017), pp. 1472–1501.

[6] L. Borcea, J. Garnier, and K. Sølna, *Wave propagation and imaging in moving random media*, SIAM Multiscale Model. Simul., 17 (2019), pp. 31–67.

[7] L. Borcea, J. Garnier, and D. Wood, *Transport of power in random waveguides with turning points*, Commun. Math. Sci., (2017), pp. 2327–2371.

[8] R. E. Collin, *Field Theory of Guided Waves*, 2nd ed., IEEE Press, Piscataway, NJ, 1990.

[9] J. Coltman, *Jet behavior in the flute*, J. Acoust. Soc. Amer., 92 (1992), pp. 74–83.

[10] J.-P. Fouque, J. Garnier, G. Papanicolaou, and K. Sølna, *Wave Propagation and Time Reversal in Randomly Layered Media*, Springer, New York, 2007.

[11] E. Franchi and M. Jacobson, *Ray propagation in a channel with depth-variable sound speed and current*, J. Acoust. Soc. Amer., 52 (1972), pp. 316–331.
[12] J. Fredberg, M. Wohl, G. Glass, and H. Dorkin, *Airway area by acoustic reflections measured at the mouth*, J. Appl. Physiol., 48 (1980), pp. 749–758.
[13] J. Garnier and G. Papanicolaou, *Pulse propagation and time reversal in random waveguides*, SIAM J. Appl. Math., 67 (2007), pp. 1718–1739.
[14] J. Garnier and K. Sølna, *Effective transport equations and enhanced backscattering in random waveguides*, SIAM J. Appl. Math., 68 (2008), pp. 1574–1599.
[15] C. Gomez, *Time-reversal superresolution in random waveguides*, SIAM Multiscale Model. Simul., 7 (2009), pp. 1348–1386.
[16] C. Gomez, *Wave propagation in underwater acoustic waveguides with rough boundaries*, Commun. Math. Sci., 13 (2015), pp. 2005–2052.
[17] N. Grigorieva, *The effect of ocean current on sound propagation*, J. Comput. Acoust., 2 (1994), pp. 441–451.
[18] R. Henrick, W. Siegmann, and M. Jacobson, *General analysis of ocean eddy effects for sound transmission applications*, J. Acoust. Soc. Amer., 62 (1977), pp. 860–870.
[19] W. Kohler and G. Papanicolaou, *Wave propagation in randomly inhomogeneous ocean*, in Wave Propagation and Underwater Acoustics, J. B. Keller and J. S. Papadakis, eds., Springer-Verlag, New York, 1977, pp. 153–223.
[20] R. Lhermitte and U. Lemmin, *Open-channel flow and turbulence measurement by high-resolution doppler sonar*, J. Atmos. Oceanic Tech., 11 (1994), pp. 1295–1308.
[21] W. Magnus, *On the exponential solution of differential equations for a linear operator*, Commun. Pure Appl. Math., 7 (1954), pp. 649–673.
[22] R. Minhong and K. Yang-Hann, *Narrowband noise attenuation characteristics of in-duct acoustic screens*, J. Sound Vib., 234 (2000), pp. 737–759.
[23] B. R. Munson, D. F. Young, T. H. Okiishi, and W. W. Huebsch, *Fundamentals of Fluid Mechanics*, 6th ed., Wiley, Hoboken, NJ, 2009.
[24] V. E. Ostashev and D. K. Wilson, *Acoustics in Moving Inhomogeneous Media*, CRC Press, Boca Raton, FL, 2015.
[25] R. Pedersen and M. Norton, *Quantification of acoustic and hydrodynamic fields in flow duct systems*, Appl. Acoust., 50 (1997), pp. 205–230.
[26] S. Percival, J. Knapp, D. Wales, and R. Edyvean, *The effect of turbulent flow and surface roughness on biofilm formation in drinking water*, J. Indust. Microbiol. Biotech., 22 (1999), pp. 152–159.
[27] R. Pinkel, *Doppler sonar observations of internal waves: The wavenumber-frequency spectrum*, J. Phys. Oceanogr., 14 (1984), pp. 1249–1270.
[28] S. Richardson, *On the no-slip boundary condition*, J. Fluid Mech., 59 (1973), pp. 707–719.
[29] O. Rodriguez and R. Oliemans, *Experimental study on oil–water flow in horizontal and slightly inclined pipes*, Internat. J. Multiphase Flow, 32 (2006), pp. 323–343.
[30] S. Thwaites and N. Fletcher, *Acoustic admittance of organ pipe jets*, J. Acoust. Soc. Amer., 74 (1983), pp. 400–408.
[31] C. Tsogka, D. A. Mitsoudis, and S. Papadimitropoulos, *Partial-aperture array imaging in acoustic waveguides*, Inverse Problems, 32 (2016), 125011.